

# Unlocking new regimes in fractional quantum Hall effect with quaternions

Mytraya Gattu and J. K. Jain

*Department of Physics, 104 Davey Lab, Pennsylvania State University, University Park, Pennsylvania 16802, USA*

(Dated: December 16, 2024)

We demonstrate that formulating the composite-fermion theory of the fractional quantum Hall (FQH) effect in terms of quaternions greatly expands its reach and opens the door into many interesting issues that were previously beyond the reach of quantitative theoretical investigation. As an illustration, we investigate the possibility of a nematic or a charge-density wave instability of the composite-fermion Fermi sea at half-filled Landau level and of the nearby FQH states by looking for a magneto-roton instability. Our quaternion formulation of the FQH effect has been inspired by mathematical developments in the theoretical analyses of gravitational wave modes and cosmic microwave background radiation, where an important role is played by spin-weighted spherical harmonics which are nothing but monopole harmonics appearing in the spherical geometry for the FQH effect.

The fractional quantum Hall (FQH) effect [1] provides an example of a strongly correlated system for which an extremely accurate microscopic understanding has been achieved in terms of the composite fermions (CFs) which experience a reduced magnetic field [2–4]. The Jain CF wave functions for electrons at filling factor  $\nu$  are constructed from the known wave functions of noninteracting electrons at filling factor  $\nu^*$  [related by  $\nu = \nu^*/(2p\nu^* \pm 1)$ ] by attaching  $2p$  vortices followed by projection into the lowest Landau level (LLL). The LLL projection was initially carried out by a brute force expansion of the unprojected wave functions in the Fock basis [5, 6]. However, this could be accomplished for very small systems because the dimension of the Fock basis grows (super) exponentially with the number of electrons ( $N$ ) and soon becomes larger than what can be stored on a computer. For the same reason, exact diagonalization (ED) studies are also typically restricted to systems with  $N \leq 16$  electrons. These allowed theoretical study of FQH states at  $\nu = 1/3, 2/3, 2/5, 3/5$  [because, it requires larger and larger systems to construct states with larger  $n$  along  $\nu = n/(2n + 1)$ .]

In a significant leap, Jain and Kamilla (JK) [7, 8] introduced an ansatz for the LLL projected wave function which does not require expansion into Fock space basis functions and allows study of systems with up to 100-200 CFs over a large range of filling factors. Extensive tests against ED studies showed these wave functions to be remarkably accurate [7–10]. The JK approach enabled detailed comparisons between theory and experiment for numerous quantities which include: energy gaps [11–14], energies of neutral magneto-roton modes [15–23], spin or valley polarization transitions [24–32], competition between FQH liquid and crystal as a function of the filling factor and Landau level (LL) mixing [33–37], Halperin-Lee-Read (HLR) Fermi sea at  $\nu = 1/2$  [38–43], pairing instability of the HLR Fermi sea and even denominator FQH effect (FQHE) [44–53], phase diagram of bilayer FQHE [46, 50, 54–61], scanning tunneling microscopy of FQH states [62–66], entanglement [67–69], etc. The JK approach also has limitations: its computational accuracy and speed diminish as we go to larger  $n$  along the

Jain  $\nu = n/(2n + 1)$  states. As a result, accurate predictions from this method are restricted in practice to states in the range  $-5 \leq n \leq 7$ .

We report in this Letter the next leap, which has been inspired by parallel developments in the fields of gravitational waves and cosmic microwave background radiation, where a generalization of the spherical harmonics called spin-weighted spherical harmonics (SWSHs) [70, 71] play an essential role. Of particular relevance here is Boyle’s work, wherein he showed that representing the SWSHs in terms of quaternions greatly simplifies the theoretical analysis [72]. Though not widely appreciated, the SWSHs are nothing but the monopole harmonics [73–75] of Haldane’s spherical geometry [76] used in the studies of the FQHE. We show that a quaternion formulation of the Jain FQH states suggests a strategy for accurate and efficient evaluation that dramatically enlarges the parameter space where reliable results may be obtained within the CF theory. With the quaternion formulation, we are able to investigate the Jain  $\nu = n/(2n + 1)$  FQH states for at least  $-20 \leq n \leq 20$  for systems containing more than 400 electrons. We show below results for  $N = 390$  particles at  $\nu = 15/31$ , whose Fock basis has a dimension of  $\sim 10^{236}$ .

As an illustration of our new method, we address whether the FQHE at  $\nu = n/(2n \pm 1)$  at large  $n$  or the HLR Fermi sea at  $\nu = 1/2$  is unstable to a charge density wave or a nematic phase [77–81]. For this purpose, we evaluate the dispersions of the neutral magneto-roton modes, modeled as CF excitons [5, 16] shown schematically in Fig. 1, for states up to  $\nu = 15/31$ . Our study brings out interesting features in the dispersion and demonstrates an extraordinary robustness of the FQHE along  $n/(2n + 1)$ , in agreement with experiments that reveal more and more Jain fractions as the sample quality is enhanced [52, 82, 83]. Furthermore, our study does not find any evidence for instability of the HLR Fermi sea at  $\nu = 1/2$ .

In Haldane’s spherical geometry, electrons are confined to move on the surface  $\mathcal{S}$  of a sphere, with a magnetic monopole of strength  $Q$  located at its center. This monopole generates a uniform radial magnetic field of

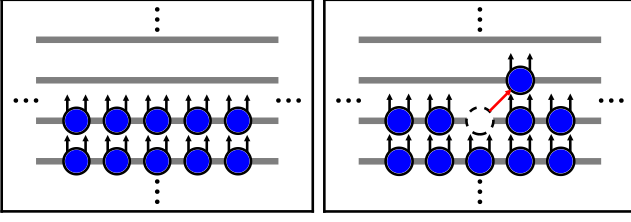


FIG. 1. The schematic on the left illustrates an incompressible state of composite fermions (CFs), depicted as electrons decorated with two flux quanta, at filling factor  $\nu = n/(2n + 1)$ , containing  $n$  fully occupied CF LLs. The schematic on the right depicts the CF exciton at  $\nu = n/(2n + 1)$ , which is the lowest energy neutral excitation.

magnitude  $B = 2Q\phi_0/(4\pi R^2)$  and produces a magnetic flux of  $2Q\phi_0$  through the surface  $\mathcal{S}$ , where  $\phi_0 = hc/e$  is called the flux quantum. The single-particle wave functions in this geometry are the monopole harmonics

$$Y_{Q,l,m}(\theta, \phi) = N_{Q,l,m}(-1)^{l-m}v^{Q-m}u^{Q+m} \times \sum_s (-1)^s \binom{l-Q}{s} \binom{l+Q}{l-m-s} (v^*v)^{l-Q-s} (u^*u)^s \quad (1)$$

$$N_{Q,l,m} = \sqrt{[(2l+1)/4\pi] \times [(\binom{2l}{l+Q})/(\binom{2l}{l+m})]}$$

Here  $l = |Q| + n_l$  is the angular momentum,  $m = -l, -l+1, \dots, l$  is the azimuthal quantum number i.e. the  $L_z$  eigenvalue,  $n_l = 0, 1, \dots$  is the LL index,  $\Omega = (\theta, \phi)$  denotes the electron's position in spherical coordinates, and  $u = \cos(\theta/2)e^{i\phi/2}$  and  $v = \sin(\theta/2)e^{-i\phi/2}$  are the spinor variables.

The monopole harmonics  $Y_{Q,l,m}$  furnish a projective representation of the three-dimensional rotational symmetry on  $\mathcal{S}$ . Under an active rotation  $\mathcal{R}$  defined by the Euler angles  $\alpha, \beta, \gamma$  (about the  $z - y - z$  axes), the monopole harmonics at  $(\theta, \phi)$  can be related to the monopole harmonics at  $(\theta', \phi')$  (where  $(\theta, \phi)$  goes to  $(\theta', \phi')$  under the rotation) as follows [72–74]

$$Y_{Q,l,m}(\theta', \phi') = e^{-iQ\psi'} \sum_{m'=-l}^l (-1)^{m-m'} [D_{m,m'}^l(\alpha, \beta, \gamma)]^* Y_{Q,l,m'}(\theta, \phi) \quad (2)$$

Here,  $D_{m,m'}^l(\alpha, \beta, \gamma)$  is the unitary Wigner- $D$  matrix corresponding to  $\mathcal{R}$  [84, 85]. The phase  $\psi'$  is a function of both  $\mathcal{R}$  and  $(\theta, \phi)$  [72, 74]; although it may be explicitly evaluated, its discontinuous nature makes it challenging to exploit the rotational symmetry on  $\mathcal{S}$  in both analytical and numerical calculations, as discussed in the Supplementary Materials (SM) [86]. To overcome this, Boyle [72] proposed an ingenious re-definition of the monopole harmonics as functions of unit quaternions that transform ordinarily under rotations and more generally under quaternion multiplication.

We begin by recalling the essential properties of quaternions. A quaternion  $r \equiv (r_0, r_1, r_2, r_3)$ , where  $r_0, r_1, r_2, r_3 \in \mathbb{R}$ , is expressed as  $r = r_0\mathbf{1} + r_1\mathbf{i} + r_2\mathbf{j} + r_3\mathbf{k}$ . The basis elements  $\mathbf{1}, \mathbf{i}, \mathbf{j}, \mathbf{k}$  correspond to the Pauli matrices  $\sigma_0, i\sigma_3, i\sigma_2, i\sigma_1$ . The rules for quaternion addition and multiplication follow from those of the basis elements, i.e., the Pauli matrices. The inverse of a (non-zero) quaternion is defined in terms of its conjugate  $r^* \equiv (r_0, -r_1, -r_2, -r_3)$  and norm  $\|r\| \equiv \sqrt{r^* \cdot r} = \sqrt{r_0^2 + r_1^2 + r_2^2 + r_3^2}$  as  $r^{-1} = r^*/\|r\|^2$ .

We now specialize to the set of unit quaternions given by  $\{r|(r_0, r_1, r_2, r_3) \in \mathbb{R}^4 \ni r_0^2 + r_1^2 + r_2^2 + r_3^2 = 1\}$  which is isomorphic to  $\mathbb{S}^3$ . We can parameterize  $r$  as

$$r = e^{\phi\mathbf{k}/2} e^{\theta\mathbf{j}/2} e^{\psi\mathbf{k}/2} = \cos \frac{\theta}{2} \cos \frac{\phi + \psi}{2} \mathbf{1} - \sin \frac{\theta}{2} \sin \frac{\phi - \psi}{2} \mathbf{i} + \sin \frac{\theta}{2} \cos \frac{\phi - \psi}{2} \mathbf{j} + \cos \frac{\theta}{2} \sin \frac{\phi + \psi}{2} \mathbf{k} \quad (3)$$

where  $(\theta, \phi, \psi)$  are the three angular coordinates on  $\mathbb{S}^3$ .

We now define, following Boyle,

$$\mathcal{Y}_{Q,l,m}(r) = Y_{Q,l,m}(u \rightarrow r_S, v \rightarrow r_A) \quad (4)$$

where  $r_S$  and  $r_A$ , the symmetric and anti-symmetric projections of  $r$ , are defined as

$$\begin{aligned} r_S &= (r + \mathbf{k} \cdot r \cdot \mathbf{k}^{-1})/2 = r_0 + r_3\mathbf{k} \\ &= \cos(\theta/2)e^{\mathbf{k}(\phi+\psi)/2} \\ r_A &= (r - \mathbf{k} \cdot r \cdot \mathbf{k}^{-1})/2 = r_2 + r_1\mathbf{k} \\ &= \sin(\theta/2)e^{\mathbf{k}(\psi-\phi)/2} \end{aligned} \quad (5)$$

(Within the sub-algebra generated by  $\mathbf{1}$  and  $\mathbf{k}$ ,  $\mathbf{k}$  behaves exactly like  $i$  i.e.  $[\mathbf{1}, \mathbf{k}] = 0$  and  $\mathbf{k}^2 = -\mathbf{1}$ . We will use  $\mathbf{k}$  and  $i$  interchangeably whenever the context is clear.) It is also useful to define another function  $\mathcal{D}_{m,m'}^l(r) = \sqrt{4\pi/(2l+1)}\mathcal{Y}_{m',l,m}(r)$  that extends the Wigner- $D$  matrices to the space of unit quaternions. We can verify from Eq. 1, that

$$\begin{aligned} \mathcal{Y}_{Q,l,m}(r) &= e^{iQ\psi} Y_{Q,l,m}(\theta, \phi) \\ \mathcal{D}_{m,m'}^l(r) &= D_{m',m}^l(-\psi, \theta, -\phi). \end{aligned} \quad (6)$$

From the transformation of the projections  $r_S$  and  $r_A$  under multiplication,

$$(r \cdot s)_S = r_S s_S - r_A^* s_A, \quad (r \cdot s)_A = r_A s_S + r_S^* s_A, \quad (7)$$

it can be shown that both  $\mathcal{D}_{m,m'}^l(r)$  and  $\mathcal{Y}_{Q,l,m}(r)$  obey

the following transformation rule

$$\begin{aligned} \mathcal{D}_{m,m'}^l(r) &= \sum_{m''=-l}^l \mathcal{D}_{m,m''}^l(r \cdot s^{-1}) \mathcal{D}_{m'',m'}^l(s) \\ \mathcal{Y}_{Q,l,m}(r) &= \sum_{m'=-l}^l \mathcal{D}_{m,m'}^l(r \cdot s^{-1}) \mathcal{Y}_{Q,l,m'}(s) \end{aligned} \quad (8)$$

which contains no phase factor! That is,  $\mathcal{Y}_{Q,l,m}(r)$  transform ordinarily under (unit) quaternion multiplication (which would be referred to as rotation below, as it connects two points on  $\mathbb{S}^3$ ). This simple behavior under rotation will play a crucial role below.

We now show that the quaternion formulation dramatically enlarges the range of FQH states that are accessible to quantitative study within CF theory. Let us recall the basic principle of the CF theory. It first prepares a state of  $N$  electrons at an effective flux  $2Q^* = 2Q - 2(N-1)$ , which in the simplest cases is given by a Slater determinant  $\det[Y_{Q^*,l_j,m_j}(\Omega_i)]$ , where  $\Omega_i$  is the position of the  $i^{\text{th}}$  electron. We then multiply it by  $\prod_{j < k=1}^N (u_j v_k - u_k v_j)^2$ , which attaches 2 vortices to each electron to convert it into a CF. Finally, this product must be projected into the LLL, which is conveniently accomplished à la the JK projection, which makes the ansatz:

$$\begin{aligned} \text{P}_{\text{LLL}} \left\{ \det [Y_{Q^*,l_j,m_j}(\Omega_i)] \prod_{j < k=1}^N (u_j v_k - u_k v_j)^2 \right\} \\ = \det [\text{P}_{\text{LLL}} Y_{Q^*,l_j,m_j}(\Omega_i) J_i] \end{aligned} \quad (9)$$

where  $\text{P}_{\text{LLL}}$  is the LLL projection operator and  $J_i = \prod_{k \neq i} (u_i v_k - u_k v_i)$ . In other words, instead of projecting the full wave function, we separately project each element of a determinant. Note that in  $Y_{Q^*,l_j,m_j}(\Omega_i) J_i$  only one (the  $i^{\text{th}}$ ) electron can be outside the LLL, thereby simplifying LLL projection.

Traditionally, the JK projection is carried out as [3, 7],

$$\begin{aligned} \text{P}_{\text{LLL}} Y_{Q^*,l,m}(\Omega_i) J_i \propto \sum_{s=0}^{l-Q^*} (-1)^s \binom{l-Q^*}{s} \times \\ \binom{Q^*+l}{l-m-s} u_i^{Q^*+m+s} v_i^{l-m-s} \partial_{u_i}^s \partial_{v_i}^{l-Q^*-s} J_i \end{aligned} \quad (10)$$

Substituting in Eq. 9 yields the CF Slater determinant state. A limiting factor of this approach is the computation of  $(l_{\text{max}} - Q^* + 1)(l_{\text{max}} - Q^* + 2)/2$  number of mixed derivatives [where  $l_{\text{max}}$  is the maximum angular momentum of an electron in  $\det Y_{Q^*,l_j,m_j}(\Omega_i)$ ], which, combined with the numerical instability in their computation [30], renders this approach unsuitable for systems with  $n \geq 8$  (i.e.  $l_{\text{max}} - Q^* = 8$ ) or  $\nu \geq 8/17$  (see SM [86] for more details). We will now see how this limitation can be overcome by a new approach to JK projection which naturally follows from the quaternion extension of JK projected wave functions.

Remembering that any physical wave function

$\Psi(\Omega_1, \dots, \Omega_N)$  can be written in terms of monopole harmonics at a given  $Q$ , Eq. 6 implies that the quaternion extension of  $\Psi$  can be written as  $\Psi(\Omega_1, \dots, \Omega_N) = \exp[-iQ(\sum_i \psi_i)] \Psi(r_1, \dots, r_N)$ , where  $\Psi(r_1, \dots, r_N)$  (here,  $r_i = e^{\phi_i \mathbf{k}/2} e^{\theta_i \mathbf{j}/2} e^{\psi_i \mathbf{k}/2}$ ) is obtained from  $\Psi(\Omega_1, \dots, \Omega_N)$  by replacing  $Y_{Q,l,m}(\Omega_i)$  with  $\mathcal{Y}_{Q,l,m}(r_i)$ . In other words, Eq. 6 implies that the extra degrees of freedom  $\psi_i$ , introduced when we extend our wave functions from  $\mathbb{S}^2$  to  $\mathbb{S}^3$ , *do not contribute to any physical observable*. What we gain by extending to quaternions—beyond the simplification of transformations under rotations—is the insight that the ubiquitous Jastrow factor  $u_i v_j - v_i u_j$  which maps into  $d(r_i, r_j) = r_i s r_j A - r_i A r_j S = (r_i^{-1} \cdot r_j)_A$ , can be regarded as a quaternion displacement that is invariant under (left) quaternion multiplication! We can exploit this invariance to evaluate  $\text{P}_{\text{LLL}} \mathcal{Y}_{Q^*,l,m}(r_i) \prod_{j \neq i} d(r_i, r_j)$  which appears in the quaternion extension of Eq. 9, as  $\sum_{m'} \mathcal{D}_{m,m'}^l(r^{-1}) \text{P}_{\text{LLL}} \mathcal{Y}_{Q^*,l,m'}(r \cdot r_i) \prod_{j \neq i} d(r \cdot r_i, r \cdot r_j)$  for arbitrary  $r$ . This allows us to rotate the system to bring the  $i^{\text{th}}$  electron to a convenient point, perform LLL projection, and rotate back. The crucial observation underlying our new approach is that the LLL projection is especially simple and efficient at  $r_i = \mathbf{1}$  which naturally suggests the choice  $r = r_i^{-1}$  and allows us to write the elements in the determinant of the JK projected wave functions as (see SM [86] for a detailed derivation):

$$\begin{aligned} \text{P}_{\text{LLL}} \mathcal{Y}_{Q^*,l,m}(r_i) \prod_{j \neq i} d(r_i, r_j) \\ = \sum_{m'=Q^*}^l (-1)^{m'-Q^*} N_{m',Q^*,Q_1}^l \mathcal{D}_{m,m'}^l(r_i) \\ \times \tilde{e}_{m'-Q^*}(\{(r_i^{-1} \cdot r_j)_S / (r_i^{-1} \cdot r_j)_A\}_{j \neq i}) \prod_{j \neq i} d(r_i, r_j) \\ N_{m',Q^*,Q_1}^l = \frac{\binom{2Q_1}{l-Q^*} \binom{l-Q^*}{m'-Q^*}}{\binom{2Q_1+l+Q^*+1}{l-Q^*}} \sqrt{\frac{(2l+1)}{4\pi} \frac{\binom{2l}{l+Q^*}}{\binom{2l}{l+m'}}} \end{aligned} \quad (11)$$

Here,  $Q_1 = (N-1)/2$  and  $\tilde{e}_{m'-Q^*}$  is the elementary symmetric polynomial [87] of degree  $m' - Q^*$  in the  $N-1$  variables  $\{(r_i^{-1} \cdot r_j)_S / (r_i^{-1} \cdot r_j)_A\}_{j \neq i}$  divided by  $\binom{N-1}{m'-Q^*}$ . The key advantage of our new approach is that the computation of all the required elementary symmetric polynomials which is the rate limiting step, scales only as  $l_{\text{max}} - Q^*$  and is robust to numerical instability [88]. This significantly increases both the computational speed and accuracy (further enhanced by the method proposed in Ref. [89]) of the JK projected wave functions, making it possible to study FQH systems containing hundreds of electrons between fillings  $1/3 \leq \nu \leq 20/41$  and  $20/39 \leq \nu \leq 2/3$  (see SM [86] for more details).

As a first application of our method, we look for a magneto-roton instability of the FQHE at  $\nu = n/(2n+1)$  as we approach  $\nu = 1/2$ . While the CF theory pre-

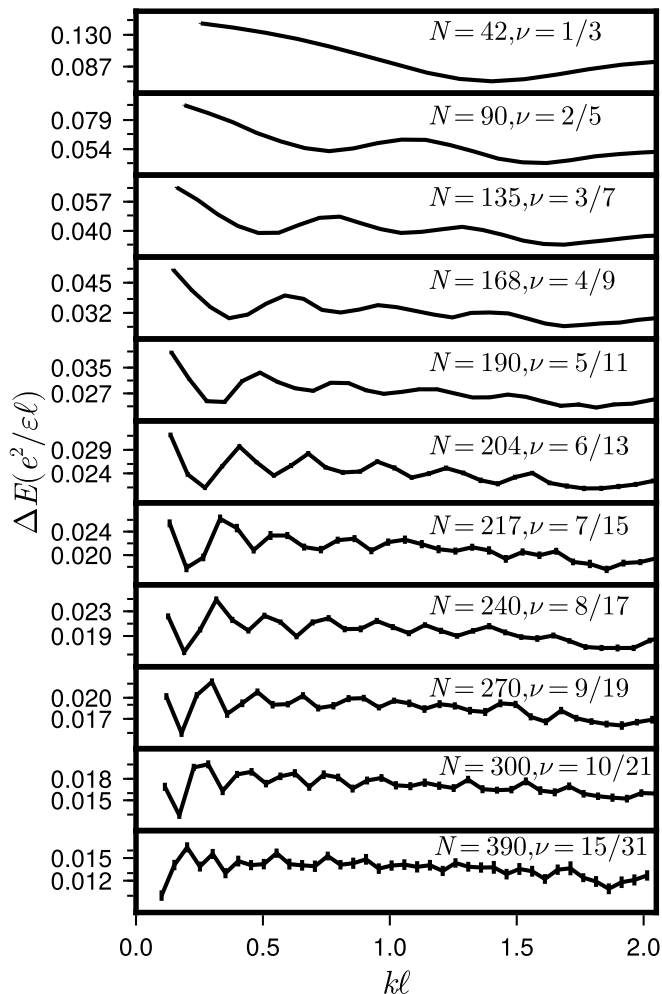


FIG. 2. The plots show the excitation energies  $\Delta E$  of the lowest neutral magneto-roton modes as a function of the wave vector  $k$  for the Jain FQH states at filling factors  $\nu = n/(2n+1)$ , obtained using our new method. The system size  $N$  and the filling factor  $\nu$  are shown on each panel. The energies are for a two-dimensional system, given in units of  $e^2/\varepsilon\ell$ , where  $\ell = \sqrt{\hbar c/eB}$  is the magnetic length. The Monte Carlo uncertainty in  $\Delta E$  is indicated by vertical bars.

dicts the possibility of FQHE at all fractions of the form  $\nu = n/(2pn \pm 1)$ , detailed calculations and comparisons with experiments are required to ascertain whether the Coulomb interaction stabilizes these states. [The Coulomb interaction fails to stabilize the  $n/(2pn \pm 1)$  states for very large  $2p$  in the LLL or for any  $2p$  in high LLs.] The FQHE along  $\nu = n/(2n+1)$  would survive to arbitrary high  $n$  if the CFs were completely non-interacting, but the CFs do have a residual interaction between them, which can, in principle, cause an instability when the interaction strength is comparable to the gap.

Remarkably, through its explicit wave functions, the CF theory also provides an accurate account of the residual CF-CF interaction and can, in principle, reveal an in-

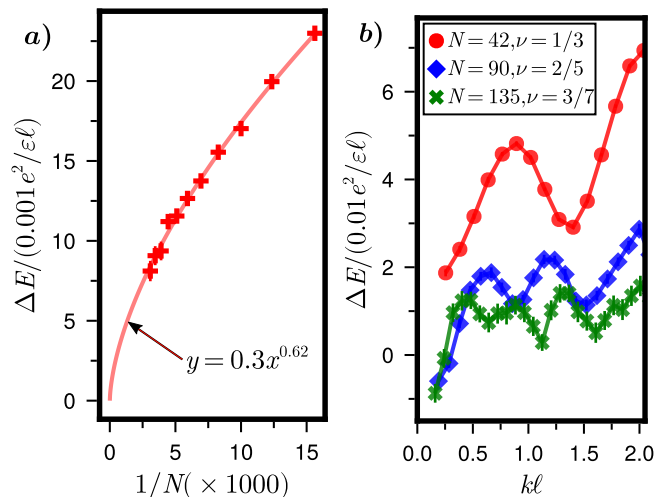


FIG. 3. a) Excitation energy  $\Delta E$  of the  $k \rightarrow 0$  CF exciton for filled shell states of CFs at  $Q^* = 0$ . The state with  $n$  filled shells has  $N = n^2$  CFs. For all systems considered here ( $n = 8, 9, \dots, 18 \Leftrightarrow N = 64, 81, \dots, 324$ ), the  $k \rightarrow 0$  CF exciton is also the lowest energy excitation. b) Excitation energy  $\Delta E$  of CF excitons as a function of  $k\ell$  for Jain FQH states at  $\nu = 1/3, 2/5, 3/7$  in the second LL.

stability. We ask here if the FQHE along  $\nu = n/(2n+1)$  is destabilized by the softening of the neutral magneto-roton excitation[90], accurately described as a CF exciton (a CF particle-hole pair) [5, 16, 91]. Fig. 2 shows the magneto-roton dispersions for several fractions, including for  $\nu = 15/31$ . (We have not made here a serious effort to achieve the largest  $n$  or  $N$ .) These dispersions show a rich structure appearing in the form of  $n$  approximately equally-spaced minima (except at  $\nu = 15/31$ , where larger systems would be needed to identify all minima), as predicted by field theoretical treatments of CFs [92–95], but no instability is encountered. Note that the first minimum occurs at  $k\ell \rightarrow 0$  [91], and the last at  $k\ell \rightarrow 2$ , which is equivalent to  $k = 2k_F$  at  $\nu = 1/2$  (where  $k_F = 1/\ell$ ).

If the magneto-roton energy were to become negative for  $\nu = n/(2n+1)$  at some large  $n$ , that would imply a similar behavior for the CF Fermi sea at  $\nu = 1/2$ . The CF Fermi sea is obtained for CFs at  $Q^* = 0$  in the limit  $N \rightarrow \infty$ . We consider systems with  $n$  filled angular momentum shells with  $N = n^2$  particles. For  $n \geq 8$ , the  $k\ell \rightarrow 0$  magneto-roton has the lowest energy; should its energy become negative, that would indicate a nematic instability [77, 79–81]. Fig. 3a shows that its energy approaches zero (rather than a negative value) in the limit of  $N \rightarrow \infty$ , and thus does not indicate any instability of the CF Fermi sea. These calculations demonstrate that FQHE remains surprisingly robust along the Jain sequence  $\nu = n/(2n+1)$ . As a demonstration of the non-triviality of these results, we plot in Fig. 3b the CF exciton dispersion at certain fractions in the second LL (of GaAs system), where we use the effective interac-

tion given in Ref. [53] to mimic the second LL. Here, an instability is seen at  $\nu = 2/5, 3/7$  etc. We note that the Jain wave functions are not very accurate representations of the exact states in the second LL, and thus our conclusions are less reliable than those in the LLL. Nonetheless, the instability of the Jain  $2/5$  state in the second LL is consistent with studies that point to the

Read-Rezayi state here [96–101]. No FQHE has been observed at  $3/7, 4/9, \dots$  in the second LL.

We thank Ajit Balram and Steven Kivelson for illuminating discussions. Computations for this research were performed on the Pennsylvania State University’s Institute for Computational and Data Sciences’ Roar Collab supercomputer. Plots were made using Makie [102].

- 
- [1] D. C. Tsui, H. L. Stormer, and A. C. Gossard. Two-dimensional magnetotransport in the extreme quantum limit. *Phys. Rev. Lett.*, 48:1559–1562, May 1982. doi:10.1103/PhysRevLett.48.1559. URL <http://link.aps.org/doi/10.1103/PhysRevLett.48.1559>.
- [2] J. K. Jain. Composite-fermion approach for the fractional quantum Hall effect. *Phys. Rev. Lett.*, 63:199–202, Jul 1989. doi:10.1103/PhysRevLett.63.199. URL <http://link.aps.org/doi/10.1103/PhysRevLett.63.199>.
- [3] J. K. Jain. *Composite Fermions*. Cambridge University Press, New York, US, 2007.
- [4] Bertrand I Halperin and Jainendra K Jain, editors. *Fractional Quantum Hall Effects New Developments*. World Scientific, 2020. doi:10.1142/11751. URL <https://worldscientific.com/doi/abs/10.1142/11751>.
- [5] Gautam Dev and J. K. Jain. Band structure of the fractional quantum Hall effect. *Phys. Rev. Lett.*, 69:2843–2846, Nov 1992. doi:10.1103/PhysRevLett.69.2843. URL <http://link.aps.org/doi/10.1103/PhysRevLett.69.2843>.
- [6] X. G. Wu, G. Dev, and J. K. Jain. Mixed-spin incompressible states in the fractional quantum hall effect. *Physical Review Letters*, 71(1):153–156, July 1993. ISSN 0031-9007. doi:10.1103/physrevlett.71.153. URL <http://dx.doi.org/10.1103/PhysRevLett.71.153>.
- [7] J. K. Jain and R. K. Kamilla. Composite fermions in the Hilbert space of the lowest electronic Landau level. *Int. J. Mod. Phys. B*, 11(22):2621–2660, 1997. doi:10.1142/S0217979297001301.
- [8] J. K. Jain and R. K. Kamilla. Quantitative study of large composite-fermion systems. *Phys. Rev. B*, 55:R4895–R4898, Feb 1997. doi:10.1103/PhysRevB.55.R4895. URL <http://link.aps.org/doi/10.1103/PhysRevB.55.R4895>.
- [9] Ajit C. Balram, Arkadiusz Wójs, and Jainendra K. Jain. State counting for excited bands of the fractional quantum Hall effect: Exclusion rules for bound excitons. *Phys. Rev. B*, 88:205312, Nov 2013. doi:10.1103/PhysRevB.88.205312. URL <http://link.aps.org/doi/10.1103/PhysRevB.88.205312>.
- [10] J. K. Jain. Thirty Years of Composite Fermions and Beyond. In B. I. Halperin and J. K. Jain, editors, *Fractional Quantum Hall Effects: New Developments*, chapter 1, pages 1–78. World Scientific Pub Co Inc, Singapore, 2020. doi:10.1142/9789811217494\_0001. URL [https://www.worldscientific.com/doi/abs/10.1142/9789811217494\\_0001](https://www.worldscientific.com/doi/abs/10.1142/9789811217494_0001).
- [11] R. R. Du, H. L. Stormer, D. C. Tsui, L. N. Pfeiffer, and K. W. West. Experimental evidence for new particles in the fractional quantum Hall effect. *Phys. Rev. Lett.*, 70:2944–2947, May 1993. doi:10.1103/PhysRevLett.70.2944. URL <http://link.aps.org/doi/10.1103/PhysRevLett.70.2944>.
- [12] H. C. Manoharan, M. Shayegan, and S. J. Klepper. Signatures of a novel Fermi liquid in a two-dimensional composite particle metal. *Phys. Rev. Lett.*, 73:3270–3273, Dec 1994. doi:10.1103/PhysRevLett.73.3270. URL <http://link.aps.org/doi/10.1103/PhysRevLett.73.3270>.
- [13] K. A. Villegas Rosales, P. T. Madathil, Y. J. Chung, L. N. Pfeiffer, K. W. West, K. W. Baldwin, and M. Shayegan. Fractional quantum hall effect energy gaps: Role of electron layer thickness. *Phys. Rev. Lett.*, 127:056801, Jul 2021. doi:10.1103/PhysRevLett.127.056801. URL <https://link.aps.org/doi/10.1103/PhysRevLett.127.056801>.
- [14] Tongzhou Zhao, Koji Kudo, W. N. Faugno, Ajit C. Balram, and J. K. Jain. Revisiting excitation gaps in the fractional quantum hall effect. *Phys. Rev. B*, 105:205147, May 2022. doi:10.1103/PhysRevB.105.205147. URL <https://link.aps.org/doi/10.1103/PhysRevB.105.205147>.
- [15] A. Pinczuk, B. S. Dennis, L. N. Pfeiffer, and K. West. Observation of collective excitations in the fractional quantum Hall effect. *Phys. Rev. Lett.*, 70:3983–3986, Jun 1993. doi:10.1103/PhysRevLett.70.3983. URL <http://link.aps.org/doi/10.1103/PhysRevLett.70.3983>.
- [16] Vito W. Scarola, Kwon Park, and Jainendra K. Jain. Rotons of composite fermions: Comparison between theory and experiment. *Phys. Rev. B*, 61:13064–13072, May 2000. doi:10.1103/PhysRevB.61.13064. URL <http://link.aps.org/doi/10.1103/PhysRevB.61.13064>.
- [17] Moonsoo Kang, A. Pinczuk, B. S. Dennis, L. N. Pfeiffer, and K. W. West. Observation of multiple magnetorotons in the fractional quantum Hall effect. *Phys. Rev. Lett.*, 86:2637–2640, Mar 2001. doi:10.1103/PhysRevLett.86.2637. URL <http://link.aps.org/doi/10.1103/PhysRevLett.86.2637>.
- [18] Irene Dujovne, A. Pinczuk, Moonsoo Kang, B. S. Dennis, L. N. Pfeiffer, and K. W. West. Composite-fermion spin excitations as  $\nu$  approaches  $1/2$ : Interactions in the Fermi sea. *Phys. Rev. Lett.*, 95:056808, Jul 2005. doi:10.1103/PhysRevLett.95.056808. URL <http://link.aps.org/doi/10.1103/PhysRevLett.95.056808>.
- [19] Gunnar Möller and Steven H. Simon. Composite fermions in a negative effective magnetic field: A Monte Carlo study. *Phys. Rev. B*, 72:045344, Jul 2005. doi:10.1103/PhysRevB.72.045344. URL <http://link.aps.org/doi/10.1103/PhysRevB.72.045344>.
- [20] Igor V. Kukushkin, Jurgen H. Smet, Vito W. Scarola, Vladimir Umansky, and Klaus von Klitzing. Dispersion of the excitations of fractional

- quantum Hall states. *Science*, 324(5930):1044–1047, 2009. doi:10.1126/science.1171472. URL <http://www.sciencemag.org/content/324/5930/1044.abstract>.
- [21] Trevor D. Rhone, Dwipesh Majumder, Brian S. Dennis, Cyrus Hirjibehedin, Irene Dujovne, Javier G. Groshaus, Yann Gallais, Jainendra K. Jain, Sudhansu S. Mandal, Aron Pinczuk, Loren Pfeiffer, and Ken West. Higher-energy composite fermion levels in the fractional quantum Hall effect. *Phys. Rev. Lett.*, 106:096803, Mar 2011. doi:10.1103/PhysRevLett.106.096803. URL <http://link.aps.org/doi/10.1103/PhysRevLett.106.096803>.
- [22] Ajit C. Balram, Zhao Liu, Andrey Gromov, and Zlatko Papić. Very-high-energy collective states of partons in fractional quantum hall liquids. *Phys. Rev. X*, 12:021008, Apr 2022. doi:10.1103/PhysRevX.12.021008. URL <https://link.aps.org/doi/10.1103/PhysRevX.12.021008>.
- [23] Dwipesh Majumder and Sudhansu S. Mandal. Neutral collective modes in spin-polarized fractional quantum Hall states at filling factors  $\frac{1}{3}$ ,  $\frac{2}{5}$ ,  $\frac{3}{7}$ , and  $\frac{4}{9}$ . *Phys. Rev. B*, 90:155310, Oct 2014. doi:10.1103/PhysRevB.90.155310. URL <http://link.aps.org/doi/10.1103/PhysRevB.90.155310>.
- [24] R. R. Du, A. S. Yeh, H. L. Stormer, D. C. Tsui, L. N. Pfeiffer, and K. W. West. Fractional quantum Hall effect around  $\nu = 3/2$ : Composite fermions with a spin. *Phys. Rev. Lett.*, 75:3926–3929, Nov 1995. doi:10.1103/PhysRevLett.75.3926. URL <http://link.aps.org/doi/10.1103/PhysRevLett.75.3926>.
- [25] R. R. Du, A. S. Yeh, H. L. Stormer, D. C. Tsui, L. N. Pfeiffer, and K. W. West.  $g$  factor of composite fermions around  $\nu = 3/2$  from angular-dependent activation-energy measurements. *Phys. Rev. B*, 55:R7351–R7354, Mar 1997. doi:10.1103/PhysRevB.55.R7351. URL <http://link.aps.org/doi/10.1103/PhysRevB.55.R7351>.
- [26] K. Park and J. K. Jain. Phase diagram of the spin polarization of composite fermions and a new effective mass. *Phys. Rev. Lett.*, 80:4237–4240, May 1998. doi:10.1103/PhysRevLett.80.4237. URL <http://link.aps.org/doi/10.1103/PhysRevLett.80.4237>.
- [27] I. V. Kukushkin, K. v. Klitzing, and K. Eberl. Spin polarization of composite fermions: Measurements of the Fermi energy. *Phys. Rev. Lett.*, 82:3665–3668, May 1999. doi:10.1103/PhysRevLett.82.3665. URL <http://link.aps.org/doi/10.1103/PhysRevLett.82.3665>.
- [28] N. C. Bishop, M. Padmanabhan, K. Vakili, Y. P. Shkolnikov, E. P. De Poortere, and M. Shayegan. Valley polarization and susceptibility of composite fermions around a filling factor  $\nu = 3/2$ . *Phys. Rev. Lett.*, 98:266404, Jun 2007. doi:10.1103/PhysRevLett.98.266404. URL <http://link.aps.org/doi/10.1103/PhysRevLett.98.266404>.
- [29] Medini Padmanabhan, T. Gokmen, and M. Shayegan. Composite fermion valley polarization energies: Evidence for particle-hole asymmetry. *Phys. Rev. B*, 81:113301, Mar 2010. doi:10.1103/PhysRevB.81.113301. URL <http://link.aps.org/doi/10.1103/PhysRevB.81.113301>.
- [30] Simon C. Davenport and Steven H. Simon. Spinful composite fermions in a negative effective field. *Phys. Rev. B*, 85:245303, Jun 2012. doi:10.1103/PhysRevB.85.245303. URL <http://link.aps.org/doi/10.1103/PhysRevB.85.245303>.
- [31] Yang Liu, S. Hasdemir, J. Shabani, M. Shayegan, L. N. Pfeiffer, K. W. West, and K. W. Baldwin. Multicomponent fractional quantum Hall states with subband and spin degrees of freedom. *Phys. Rev. B*, 92:201101, Nov 2015. doi:10.1103/PhysRevB.92.201101. URL <http://link.aps.org/doi/10.1103/PhysRevB.92.201101>.
- [32] Yuhe Zhang, A. Wójs, and J. K. Jain. Landau-level mixing and particle-hole symmetry breaking for spin transitions in the fractional quantum hall effect. *Physical Review Letters*, 117(11), September 2016. ISSN 1079-7114. doi:10.1103/physrevlett.117.116803. URL <http://dx.doi.org/10.1103/PhysRevLett.117.116803>.
- [33] Alexander C. Archer, Kwon Park, and Jainendra K. Jain. Competing crystal phases in the lowest Landau level. *Phys. Rev. Lett.*, 111:146804, Oct 2013. doi:10.1103/PhysRevLett.111.146804.
- [34] Yang Liu, D. Kamburov, S. Hasdemir, M. Shayegan, L. N. Pfeiffer, K. W. West, and K. W. Baldwin. Fractional quantum Hall effect and Wigner crystal of interacting composite fermions. *Phys. Rev. Lett.*, 113:246803, Dec 2014. doi:10.1103/PhysRevLett.113.246803. URL <http://link.aps.org/doi/10.1103/PhysRevLett.113.246803>.
- [35] Jianyun Zhao, Yuhe Zhang, and J. K. Jain. Crystallization in the fractional quantum hall regime induced by landau-level mixing. *Physical Review Letters*, 121(11), September 2018. ISSN 1079-7114. doi:10.1103/physrevlett.121.116802. URL <http://dx.doi.org/10.1103/PhysRevLett.121.116802>.
- [36] K. A. Villegas Rosales, S. K. Singh, Meng K. Ma, Md. Shafayat Hossain, Y. J. Chung, L. N. Pfeiffer, K. W. West, K. W. Baldwin, and M. Shayegan. Competition between fractional quantum hall liquid and wigner solid at small fillings: Role of layer thickness and landau level mixing. *Phys. Rev. Res.*, 3:013181, Feb 2021. doi:10.1103/PhysRevResearch.3.013181. URL <https://link.aps.org/doi/10.1103/PhysRevResearch.3.013181>.
- [37] P. T. Madathil, C. Wang, S. K. Singh, A. Gupta, K. A. Villegas Rosales, Y. J. Chung, K. W. West, K. W. Baldwin, L. N. Pfeiffer, L. W. Engel, and M. Shayegan. Signatures of correlated defects in an ultraclean wigner crystal in the extreme quantum limit. *Phys. Rev. Lett.*, 132:096502, Mar 2024. doi:10.1103/PhysRevLett.132.096502. URL <https://link.aps.org/doi/10.1103/PhysRevLett.132.096502>.
- [38] B. I. Halperin, Patrick A. Lee, and Nicholas Read. Theory of the half-filled Landau level. *Phys. Rev. B*, 47:7312–7343, Mar 1993. doi:10.1103/PhysRevB.47.7312. URL <http://link.aps.org/doi/10.1103/PhysRevB.47.7312>.
- [39] E. Rezayi and N. Read. Fermi-liquid-like state in a half-filled Landau level. *Phys. Rev. Lett.*, 72:900–903, Feb 1994. doi:10.1103/PhysRevLett.72.900. URL <http://link.aps.org/doi/10.1103/PhysRevLett.72.900>.
- [40] E. H. Rezayi and F. D. M. Haldane. Incompressible paired Hall state, stripe order, and the composite fermion liquid phase in half-filled Landau levels. *Phys. Rev. Lett.*, 84:4685–4688, May 2000. doi:10.1103/PhysRevLett.84.4685. URL <http://link.aps.org/doi/10.1103/PhysRevLett.84.4685>.
- [41] Kyungmin Lee, Junping Shao, Eun-Ah Kim,

- F. D. M. Haldane, and Edward H. Rezayi. Pomeranchuk instability of composite fermi liquids. *Phys. Rev. Lett.*, 121:147601, Oct 2018. doi: 10.1103/PhysRevLett.121.147601. URL <https://link.aps.org/doi/10.1103/PhysRevLett.121.147601>.
- [42] M. Fremling, N. Moran, J. K. Slingerland, and S. H. Simon. Trial wave functions for a composite Fermi liquid on a torus. *Phys. Rev. B*, 97:035149, Jan 2018. doi:10.1103/PhysRevB.97.035149. URL <https://link.aps.org/doi/10.1103/PhysRevB.97.035149>.
- [43] Scott D. Geraedts, Jie Wang, E. H. Rezayi, and F. D. M. Haldane. Berry phase and model wave function in the half-filled Landau level. *Phys. Rev. Lett.*, 121:147202, Oct 2018. doi: 10.1103/PhysRevLett.121.147202. URL <https://link.aps.org/doi/10.1103/PhysRevLett.121.147202>.
- [44] Anirban Sharma, Ajit C. Balram, and J. K. Jain. Composite-fermion pairing at half-filled and quarter-filled lowest Landau level. *Phys. Rev. B*, 109:035306, Jan 2024. doi:10.1103/PhysRevB.109.035306. URL <https://link.aps.org/doi/10.1103/PhysRevB.109.035306>.
- [45] Greg J. Henderson, Gunnar Möller, and Steven H. Simon. Energy minimization of paired composite fermion wave functions in the spherical geometry. *Phys. Rev. B*, 108:245128, Dec 2023. doi: 10.1103/PhysRevB.108.245128. URL <https://link.aps.org/doi/10.1103/PhysRevB.108.245128>.
- [46] G. Möller and S. H. Simon. Paired composite-fermion wave functions. *Phys. Rev. B*, 77:075319, Feb 2008. doi:10.1103/PhysRevB.77.075319. URL <https://link.aps.org/doi/10.1103/PhysRevB.77.075319>.
- [47] N. Moran, A. Sterdyniak, I. Vidanović, N. Regnault, and M. V. Milovanović. Topological  $d$ -wave pairing structures in Jain states. *Phys. Rev. B*, 85:245307, Jun 2012. doi:10.1103/PhysRevB.85.245307. URL <http://link.aps.org/doi/10.1103/PhysRevB.85.245307>.
- [48] Y. W. Suen, H. C. Manoharan, X. Ying, M. B. Santos, and M. Shayegan. Origin of the  $\nu = 1/2$  fractional quantum Hall state in wide single quantum wells. *Phys. Rev. Lett.*, 72:3405–3408, May 1994. doi: 10.1103/PhysRevLett.72.3405. URL <https://link.aps.org/doi/10.1103/PhysRevLett.72.3405>.
- [49] Ajit C. Balram, Maissam Barkeshli, and Mark S. Rudner. Parton construction of a wave function in the anti-Pfaffian phase. *Phys. Rev. B*, 98:035127, Jul 2018. doi:10.1103/PhysRevB.98.035127. URL <https://link.aps.org/doi/10.1103/PhysRevB.98.035127>.
- [50] Glenn Wagner, Dung X. Nguyen, Steven H. Simon, and Bertrand I. Halperin.  $s$ -wave paired electron and hole composite fermion trial state for quantum hall bilayers with  $\nu = 1$ . *Phys. Rev. Lett.*, 127:246803, Dec 2021. doi: 10.1103/PhysRevLett.127.246803. URL <https://link.aps.org/doi/10.1103/PhysRevLett.127.246803>.
- [51] Chengyu Wang, A. Gupta, S. K. Singh, Y. J. Chung, L. N. Pfeiffer, K. W. West, K. W. Baldwin, R. Winkler, and M. Shayegan. Even-denominator fractional quantum hall state at filling factor  $\nu = 3/4$ . *Phys. Rev. Lett.*, 129:156801, Oct 2022. doi: 10.1103/PhysRevLett.129.156801. URL <https://link.aps.org/doi/10.1103/PhysRevLett.129.156801>.
- [52] Chengyu Wang, A. Gupta, S. K. Singh, P. T. Madathil, Y. J. Chung, L. N. Pfeiffer, K. W. Baldwin, R. Winkler, and M. Shayegan. Fractional quantum hall state at filling factor  $\nu = 1/4$  in ultra-high-quality GaAs two-dimensional hole systems. *Phys. Rev. Lett.*, 131:266502, Dec 2023. doi: 10.1103/PhysRevLett.131.266502. URL <https://link.aps.org/doi/10.1103/PhysRevLett.131.266502>.
- [53] Misha Yutushui and David F. Mross. Phase diagram of compressible and paired states in the quarter-filled Landau level. arXiv [cond-mat.str-el], August 2024. URL <http://dx.doi.org/10.1103/PhysRevB.92.235302>.
- [54] J. I. A. Li, Q. Shi, Y. Zeng, K. Watanabe, T. Taniguchi, J. Hone, and C. R. Dean. Pairing states of composite fermions in double-layer graphene. *Nature Physics*, 15(9):898–903, 2019. ISSN 1745-2481. doi: 10.1038/s41567-019-0547-z. URL <https://doi.org/10.1038/s41567-019-0547-z>.
- [55] Xiaomeng Liu, Zeyu Hao, Kenji Watanabe, Takashi Taniguchi, Bertrand I. Halperin, and Philip Kim. Interlayer fractional quantum Hall effect in a coupled graphene double layer. *Nature Physics*, 15(9):893–897, 2019. ISSN 1745-2481. doi:10.1038/s41567-019-0546-0. URL <https://doi.org/10.1038/s41567-019-0546-0>.
- [56] V. W. Scarola and J. K. Jain. Phase diagram of bilayer composite fermion states. *Phys. Rev. B*, 64:085313, Aug 2001. doi:10.1103/PhysRevB.64.085313. URL <http://link.aps.org/doi/10.1103/PhysRevB.64.085313>.
- [57] Gunnar Möller, Steven H. Simon, and Edward H. Rezayi. Trial wave functions for  $\nu = \frac{1}{2} + \frac{1}{2}$  quantum hall bilayers. *Phys. Rev. B*, 79:125106, Mar 2009. doi:10.1103/PhysRevB.79.125106. URL <https://link.aps.org/doi/10.1103/PhysRevB.79.125106>.
- [58] Michael P. Zaletel, Scott Geraedts, Zlatko Papić, and Edward H. Rezayi. Evidence for a topological “exciton fermi sea” in bilayer graphene. *Physical Review B*, 98(4), July 2018. ISSN 2469-9969. doi: 10.1103/physrevb.98.045113. URL <http://dx.doi.org/10.1103/PhysRevB.98.045113>.
- [59] J. I. A. Li, C. Tan, S. Chen, Y. Zeng, T. Taniguchi, K. Watanabe, J. Hone, and C. R. Dean. Even denominator fractional quantum Hall states in bilayer graphene. *Science*, 2017. ISSN 0036-8075. doi:10.1126/science.aao2521. URL <http://science.sciencemag.org/content/early/2017/10/04/science.aao2521>.
- [60] Glenn Wagner and Dung X. Nguyen. Successive electron-vortex binding in quantum hall bilayers at  $\nu = \frac{1}{4} + \frac{3}{4}$ . *Phys. Rev. B*, 110:195106, Nov 2024. doi: 10.1103/PhysRevB.110.195106. URL <https://link.aps.org/doi/10.1103/PhysRevB.110.195106>.
- [61] Qi Hu, Titus Neupert, and Glenn Wagner. Single-parameter variational wave functions for quantum hall bilayers. *Phys. Rev. B*, 109:155138, Apr 2024. doi: 10.1103/PhysRevB.109.155138. URL <https://link.aps.org/doi/10.1103/PhysRevB.109.155138>.
- [62] Yuwen Hu, Yen-Chen Tsui, Minhao He, Umut Kamber, Taige Wang, Amir S Mohammadi, Kenji Watanabe, Takashi Taniguchi, Zlatko Papić, Michael P Zaletel, and Ali Yazdani. High-resolution tunneling spectroscopy of fractional quantum hall states. arXiv preprint arXiv:2308.05789, 2023.
- [63] Jainendra K. Jain and Michael R. Peterson. Reconstructing the electron in a fractionalized quantum fluid. *Phys. Rev. Lett.*, 94:186808, May 2005. doi: 10.1103/PhysRevLett.94.186808. URL <http://link.aps.org/doi/10.1103/PhysRevLett.94.186808>.
- [64] Mytraya Gattu, G. J. Sreejith, and J. K. Jain.

- Scanning tunneling microscopy of fractional quantum hall states: Spectroscopy of composite-fermion bound states. *Phys. Rev. B*, 109:L201123, May 2024. doi: 10.1103/PhysRevB.109.L201123. URL <https://link.aps.org/doi/10.1103/PhysRevB.109.L201123>.
- [65] Songyang Pu, Ajit C. Balram, Yuwen Hu, Yen-Chen Tsui, Minhao He, Nicolas Regnault, Michael P. Zaletel, Ali Yazdani, and Zlatko Papić. Fingerprints of composite fermion lambda levels in scanning tunneling microscopy. *Physical Review B*, 110(8), August 2024. ISSN 2469-9969. doi:10.1103/physrevb.110.l081107. URL <http://dx.doi.org/10.1103/PhysRevB.110.L081107>.
- [66] Xinlei Yue and Ady Stern. Electronic excitations in the bulk of fractional quantum hall states. *Phys. Rev. B*, 110:115428, Sep 2024. doi: 10.1103/PhysRevB.110.115428. URL <https://link.aps.org/doi/10.1103/PhysRevB.110.115428>.
- [67] Iván D. Rodríguez, Steven H. Simon, and J. K. Slingerland. Evaluation of ranks of real space and particle entanglement spectra for large systems. *Phys. Rev. Lett.*, 108:256806, Jun 2012. doi: 10.1103/PhysRevLett.108.256806. URL <http://link.aps.org/doi/10.1103/PhysRevLett.108.256806>.
- [68] Simon C. Davenport, Iván D. Rodríguez, J. K. Slingerland, and Steven H. Simon. Composite fermion model for entanglement spectrum of fractional quantum Hall states. *Phys. Rev. B*, 92:115155, Sep 2015. doi: 10.1103/PhysRevB.92.115155. URL <https://link.aps.org/doi/10.1103/PhysRevB.92.115155>.
- [69] Junping Shao, Eun-Ah Kim, F. D. M. Haldane, and Edward H. Rezayi. Entanglement entropy of the  $\nu = 1/2$  composite fermion non-Fermi liquid state. *Phys. Rev. Lett.*, 114:206402, May 2015. doi: 10.1103/PhysRevLett.114.206402. URL <http://link.aps.org/doi/10.1103/PhysRevLett.114.206402>.
- [70] E. T. Newman and R. Penrose. Note on the bondi-metzner-sachs group. *Journal of Mathematical Physics*, 7(5):863–870, May 1966. ISSN 1089-7658. doi:10.1063/1.1931221. URL <http://dx.doi.org/10.1063/1.1931221>.
- [71] Kip S. Thorne. Multipole expansions of gravitational radiation. *Reviews of Modern Physics*, 52(2):299–339, April 1980. ISSN 0034-6861. doi: 10.1103/revmodphys.52.299. URL <http://dx.doi.org/10.1103/RevModPhys.52.299>.
- [72] Michael Boyle. How should spin-weighted spherical functions be defined? *Journal of Mathematical Physics*, 57(9), September 2016. ISSN 1089-7658. doi:10.1063/1.4962723. URL <http://dx.doi.org/10.1063/1.4962723>.
- [73] Tai Tsun Wu and Chen Ning Yang. Dirac monopole without strings: Monopole harmonics. *Nuclear Physics B*, 107(3):365–380, May 1976. ISSN 0550-3213. doi: 10.1016/0550-3213(76)90143-7. URL [http://dx.doi.org/10.1016/0550-3213\(76\)90143-7](http://dx.doi.org/10.1016/0550-3213(76)90143-7).
- [74] Tai Tsun Wu and Chen Ning Yang. Some properties of monopole harmonics. *Physical Review D*, 16(4):1018–1021, August 1977. ISSN 0556-2821. doi: 10.1103/physrevd.16.1018. URL <http://dx.doi.org/10.1103/PhysRevD.16.1018>.
- [75] Tevian Dray. The relationship between monopole harmonics and spin-weighted spherical harmonics. *Journal of Mathematical Physics*, 26(5):1030–1033, May 1985. ISSN 1089-7658. doi:10.1063/1.526533. URL <http://dx.doi.org/10.1063/1.526533>.
- [76] F. D. M. Haldane. Fractional quantization of the Hall effect: A hierarchy of incompressible quantum fluid states. *Phys. Rev. Lett.*, 51:605–608, Aug 1983. doi: 10.1103/PhysRevLett.51.605. URL <http://link.aps.org/doi/10.1103/PhysRevLett.51.605>.
- [77] J. Maciejko, B. Hsu, S. A. Kivelson, YeJe Park, and S. L. Sondhi. Field theory of the quantum hall nematic transition. *Physical Review B*, 88(12), September 2013. ISSN 1550-235X. doi:10.1103/physrevb.88.125137. URL <http://dx.doi.org/10.1103/PhysRevB.88.125137>.
- [78] Dung Xuan Nguyen, Andrey Gromov, and Dam Thanh Son. Fractional quantum hall systems near nematicity: Bimetric theory, composite fermions, and dirac brackets. *Phys. Rev. B*, 97:195103, May 2018. doi: 10.1103/PhysRevB.97.195103. URL <https://link.aps.org/doi/10.1103/PhysRevB.97.195103>.
- [79] Bo Yang. Microscopic theory for nematic fractional quantum hall effect. *Physical Review Research*, 2(3), September 2020. ISSN 2643-1564. doi: 10.1103/physrevresearch.2.033362. URL <http://dx.doi.org/10.1103/PhysRevResearch.2.033362>.
- [80] Yizhi You, Gil Young Cho, and Eduardo Fradkin. Theory of nematic fractional quantum hall states. *Physical Review X*, 4(4), December 2014. ISSN 2160-3308. doi: 10.1103/physrevx.4.041050. URL <http://dx.doi.org/10.1103/PhysRevX.4.041050>.
- [81] Songyang Pu, Ajit C. Balram, Joseph Taylor, Eduardo Fradkin, and Zlatko Papić. Microscopic model for fractional quantum hall nematics. *Physical Review Letters*, 132(23), June 2024. ISSN 1079-7114. doi: 10.1103/physrevlett.132.236503. URL <http://dx.doi.org/10.1103/PhysRevLett.132.236503>.
- [82] Yoon Jang Chung, K. A. Villegas Rosales, K. W. Baldwin, P. T. Madathil, K. W. West, M. Shayegan, and L. N. Pfeiffer. Ultra-high-quality two-dimensional electron systems. *Nature Materials*, Feb 2021. ISSN 1476-4660. doi:10.1038/s41563-021-00942-3. URL <https://doi.org/10.1038/s41563-021-00942-3>.
- [83] Yoon Jang Chung, D. Graf, L. W. Engel, K. A. Villegas Rosales, P. T. Madathil, K. W. Baldwin, K. W. West, L. N. Pfeiffer, and M. Shayegan. Correlated states of 2D electrons near the Landau level filling  $\nu = 1/7$ . *Phys. Rev. Lett.*, 128:026802, Jan 2022. doi: 10.1103/PhysRevLett.128.026802. URL <https://link.aps.org/doi/10.1103/PhysRevLett.128.026802>.
- [84] Eugen Wigner. *Gruppentheorie und ihre Anwendung auf die Quantenmechanik der Atomspektren*. Vieweg+Teubner Verlag, 1931. ISBN 9783663025559. doi:10.1007/978-3-663-02555-9. URL <http://dx.doi.org/10.1007/978-3-663-02555-9>.
- [85] J. J. Sakurai and Jim Napolitano. *Modern Quantum Mechanics*. Cambridge University Press, September 2020. ISBN 9781108473224. doi: 10.1017/9781108587280. URL <http://dx.doi.org/10.1017/9781108587280>.
- [86] Supplemental Materials section includes discussion of how the monopole harmonics transform under rotation, derivation of Jain-Kamilla projection in the quaternion formulation, and the particle number dependence of the magneto-roton dispersion.
- [87] Ian Grant Macdonald. *Symmetric Functions and Hall Polynomials*. Oxford: Clarendon Press, 1979.
- [88] Rizwana Rehman and Ilse C. F. Ipsen. Computing char-

- acteristic polynomials from eigenvalues. *SIAM Journal on Matrix Analysis and Applications*, 32(1):90–114, January 2011. ISSN 1095-7162. doi:10.1137/100788392. URL <http://dx.doi.org/10.1137/100788392>.
- [89] X. M. Feng, P. Wang, W. Yang, and G. R. Jin. High-precision evaluation of wigner’s  $d$  matrix by exact diagonalization. *Phys. Rev. E*, 92:043307, Oct 2015. doi:10.1103/PhysRevE.92.043307. URL <https://link.aps.org/doi/10.1103/PhysRevE.92.043307>.
- [90] S. M. Girvin, A. H. MacDonald, and P. M. Platzman. Collective-excitation gap in the fractional quantum Hall effect. *Phys. Rev. Lett.*, 54:581–583, Feb 1985. doi:10.1103/PhysRevLett.54.581. URL <http://link.aps.org/doi/10.1103/PhysRevLett.54.581>.
- [91] Ajit C. Balram, G. J. Sreejith, and J. K. Jain. Splitting of the girvin-macdonald-platzman density wave and the nature of chiral gravitons in the fractional quantum hall effect. *Phys. Rev. Lett.*, 133:246605, Dec 2024. doi:10.1103/PhysRevLett.133.246605. URL <https://link.aps.org/doi/10.1103/PhysRevLett.133.246605>.
- [92] Steven H. Simon and Bertrand I. Halperin. Finite-wave-vector electromagnetic response of fractional quantized Hall states. *Phys. Rev. B*, 48:17368–17387, Dec 1993. doi:10.1103/PhysRevB.48.17368. URL <http://link.aps.org/doi/10.1103/PhysRevB.48.17368>.
- [93] Siavash Golkar, Dung Xuan Nguyen, Matthew M. Roberts, and Dam Thanh Son. Higher-spin theory of the magnetorotons. *Phys. Rev. Lett.*, 117:216403, Nov 2016. doi:10.1103/PhysRevLett.117.216403. URL <http://link.aps.org/doi/10.1103/PhysRevLett.117.216403>.
- [94] K. Park and J. K. Jain. Two-roton bound state in the fractional quantum Hall effect. *Phys. Rev. Lett.*, 84:5576–5579, Jun 2000. doi:10.1103/PhysRevLett.84.5576. URL <http://link.aps.org/doi/10.1103/PhysRevLett.84.5576>.
- [95] Ajit C Balram and Songyang Pu. Positions of the magnetoroton minima in the fractional quantum hall effect. *The European Physical Journal B: Condensed Matter and Complex Systems*, 90(6):124, 2017.
- [96] N. Read and E. Rezayi. Beyond paired quantum Hall states: Parafermions and incompressible states in the first excited Landau level. *Phys. Rev. B*, 59:8084–8092, Mar 1999. doi:10.1103/PhysRevB.59.8084. URL <http://link.aps.org/doi/10.1103/PhysRevB.59.8084>.
- [97] Parsa Bonderson, Adrian E. Feiguin, Gunnar Möller, and J. K. Slingerland. Competing topological orders in the  $\nu = 12/5$  quantum Hall state. *Phys. Rev. Lett.*, 108:036806, Jan 2012. doi:10.1103/PhysRevLett.108.036806. URL <http://link.aps.org/doi/10.1103/PhysRevLett.108.036806>.
- [98] G. J. Sreejith, Ying-Hai Wu, A. Wójs, and J. K. Jain. Tripartite composite fermion states. *Phys. Rev. B*, 87:245125, Jun 2013. doi:10.1103/PhysRevB.87.245125. URL <http://link.aps.org/doi/10.1103/PhysRevB.87.245125>.
- [99] Cécile Repellin, Titus Neupert, B. Andrei Bernevig, and Nicolas Regnault. Projective construction of the  $F_k$  Read-Rezayi fractional quantum Hall states and their excitations on the torus geometry. *Phys. Rev. B*, 92:115128, Sep 2015. doi:10.1103/PhysRevB.92.115128. URL <https://link.aps.org/doi/10.1103/PhysRevB.92.115128>.
- [100] Bartosz Kuśmierz and Arkadiusz Wójs. Emergence of jack ground states from two-body pseudopotentials in fractional quantum Hall systems. *Phys. Rev. B*, 97:245125, Jun 2018. doi:10.1103/PhysRevB.97.245125. URL <https://link.aps.org/doi/10.1103/PhysRevB.97.245125>.
- [101] Ajit C Balram. Transitions from abelian composite fermion to non-abelian parton fractional quantum hall states in the zeroth landau level of bilayer graphene. *Physical Review B*, 105(12):L121406, 2022.
- [102] Simon Danisch and Julius Krumbiegel. Makie.jl: Flexible high-performance data visualization for julia. *Journal of Open Source Software*, 6(65):3349, September 2021. ISSN 2475-9066. doi:10.21105/joss.03349. URL <http://dx.doi.org/10.21105/joss.03349>.

# Supplementary Material for “Unlocking new regimes in fractional quantum Hall effect with quaternions”

Mytraya Gattu and J. K. Jain

Department of Physics, 104 Davey Lab, Pennsylvania State University, University Park, Pennsylvania 16802, USA

(Dated: December 16, 2024)

In Sec. I, we provide a detailed analysis of the transformation properties of monopole harmonics under rotation, when expressed in terms of the spinor variables. Specifically, we demonstrate that the phase factor they acquire under rotations is discontinuous at points mapping to the poles. In Sec. II, we derive the expression for Jain-Kamilla projection in the quaternion representation and discuss how it leads to a much more efficient evaluation of the Jain-Kamilla wave functions. Finally, in Sec. III, we provide dispersions for the magneto-roton modes at several Jain fractions.

## I. MONOPOLE HARMONICS UNDER ROTATION

Eq. 2 of the main text (Eq. 6 below), which shows how the monopole harmonics  $Y_{Q,l,m}(\theta, \phi)$  transform under rotations described by the Euler angles  $\alpha, \beta, \gamma$  about the  $z - y - z$  axes, was first derived in Ref. [1, 2]. We include an alternate derivation below for completeness and for the reader's convenience. Through examples, we show that the phase  $Q\psi'$  in Eq. 6 acquired by the monopole harmonics under a rotation is in general discontinuous at the points that go to the poles under the rotation.

In the spherical geometry, the single particle eigenstates in a uniform radial magnetic field produced by a monopole of strength  $Q$  are the monopole harmonics  $Y_{Q,l,m}(\Omega)$ . Here,  $l = |Q|, |Q| + 1, \dots$  is the angular momentum,  $m = -l, -l + 1, \dots, l$  is the azimuthal quantum number, and  $\Omega = (\theta, \phi)$  is the position in spherical coordinates. The monopole harmonics  $Y_{Q,l,m}(\theta, \phi)$  are defined as polynomials in the spinor variables  $u = \cos(\theta/2)e^{i\phi/2}$  and  $v = \sin(\theta/2)e^{-i\phi/2}$  as [1, 3]

$$Y_{Q,l,m}(\theta, \phi) = N_{Q,l,m} (-1)^{l-m} v^{Q-m} u^{Q+m} \times \sum_s (-1)^s \binom{l-Q}{s} \binom{l+Q}{l-m-s} (v^* v)^{l-Q-s} (u^* u)^s \quad (1)$$

$$N_{Q,l,m} = \sqrt{\frac{2l+1}{4\pi} \frac{(l+m)!(l-m)!}{(l+Q)!(l-Q)!}}$$

From the rotational symmetry of the spherical geometry and from general symmetry considerations [4], it follows that we should be able to write

$$Y_{Q,l,m}(\theta', \phi') = e^{i\Gamma} \sum_{m'=-l}^l U_{m,m'}^l(\mathcal{R}(\alpha, \beta, \gamma)) Y_{Q,l,m'}(\theta, \phi) \quad (2)$$

at every point  $(\theta', \phi')$  which is related to the point  $(\theta, \phi)$  by the rotation  $\mathcal{R}(\alpha, \beta, \gamma)$ . Here,  $U_{m,m'}^l(\mathcal{R}(\alpha, \beta, \gamma))$  is a unitary matrix generating the rotation and  $\Gamma$  is a phase which, in general, depends on both  $(\theta, \phi)$  and  $\mathcal{R}(\alpha, \beta, \gamma)$ . Now, the question is: Can we find an explicit form for  $U_{m,m'}^l(\mathcal{R}(\alpha, \beta, \gamma))$  and  $\Gamma$  to be able to exploit the rotational invariance?

We can in principle, relate  $Y_{Q,l,m}(\theta', \phi')$  to  $Y_{Q,l,m}(\theta, \phi)$  by expressing the spinor variables  $u' = \cos(\theta'/2)e^{i\phi'/2}$  and  $v' = \sin(\theta'/2)e^{-i\phi'/2}$  appearing in Eq. 1 in terms of the original spinor variables  $u = \cos(\theta/2)e^{i\phi/2}$  and  $v = \sin(\theta/2)e^{-i\phi/2}$ . To do so would require solving

$$\begin{pmatrix} \sin \theta' \cos \phi' \\ \sin \theta' \sin \phi' \\ \cos \theta' \end{pmatrix} = \begin{pmatrix} \cos \alpha & -\sin \alpha & 0 \\ \sin \alpha & \cos \alpha & 0 \\ 0 & 0 & 1 \end{pmatrix} \times \begin{pmatrix} \cos \beta & 0 & \sin \beta \\ 0 & 1 & 0 \\ -\sin \beta & 0 & \cos \beta \end{pmatrix} \begin{pmatrix} \cos \gamma & -\sin \gamma & 0 \\ \sin \gamma & \cos \gamma & 0 \\ 0 & 0 & 1 \end{pmatrix} \begin{pmatrix} \sin \theta \cos \phi \\ \sin \theta \sin \phi \\ \cos \theta \end{pmatrix}. \quad (3)$$

for  $\cos(\theta'/2), \sin(\theta'/2), \cos(\phi'/2)$  and  $\sin(\phi'/2)$ . Except for the most straightforward rotations (i.e., the ones about the  $z$ -axis alone), solving for the new spinor variables would require a careful consideration of branch cuts.

A more practical and insightful approach can be taken by noting that, mathematically, the monopole harmonics  $Y_{Q,l,m}(\theta, \phi)$  can be related to a row of the unitary Wigner- $D$  matrices that generate rotations in three dimensions as [1]:

$$Y_{Q,l,m}(\theta, \phi) = \sqrt{\frac{2l+1}{4\pi}} D_{Q,m}^l(0, \theta, -\phi) \quad (4)$$

Here,  $D_{m,m'}^l(\alpha, \beta, \gamma)$  is the Wigner- $D$  matrix generating an active rotation described by the Euler angles  $\alpha, \beta, \gamma$  about the  $z - y - z$  axes of a spin- $l$  particle [5]:

$$D_{m,m'}^l(\alpha, \beta, \gamma) = \langle l, m | e^{-i\alpha J_z} e^{-i\beta J_y} e^{-i\gamma J_z} | l, m' \rangle \quad (5)$$

Here,  $J_x, J_y, J_z$  are the angular momentum operators and  $\langle \theta, \phi | l, m \rangle = Y_{l,m}(\theta, \phi)$  are the spherical harmonics of angular momentum  $l$ . [We will follow the above convention for the Euler angles and refer to such rotations as  $\mathcal{R}(\alpha, \beta, \gamma)$ , with  $\mathcal{R}^{-1}(\alpha, \beta, \gamma) = \mathcal{R}(-\gamma, -\beta, -\alpha)$ .] Therefore, to relate the monopole harmonics  $Y_{Q,l,m}(\theta', \phi')$  to the monopole harmonics  $Y_{Q,l,m}(\theta, \phi)$ , all we need to do is to express the rotation  $\mathcal{R}(0, \theta', -\phi')$  in terms of the

rotation  $\mathcal{R}(0, \theta, -\phi)$ . If we can do this, we can use the transformation rule for the Wigner- $D$  matrices under the composition of rotations,  $D_{m_1, m_2}^l(\mathcal{R}_1 \cdot \mathcal{R}_2) = \sum_{m'=-l}^l D_{m_1, m'}^l(\mathcal{R}_1) D_{m', m_2}^l(\mathcal{R}_2)$  to construct the transformation rule for the monopole harmonics under rotations.

To proceed further, consider the following thought exercise. First, what does the inverse of the rotation  $\mathcal{R}(0, \theta, -\phi)$  do? Its inverse  $\mathcal{R}(\phi, -\theta, 0)$ , takes the north pole to the point  $(\theta, \pi + \phi)$ . If we now apply another rotation  $\mathcal{R}(0, 0, \pi)$ , we can bring the north pole under the combined action to  $(\theta, \phi)$ . Now, we know that, under  $\mathcal{R}(\alpha, \beta, \gamma)$ ,  $(\theta, \phi)$  goes to  $(\theta', \phi')$  and therefore, under the combined rotation  $\mathcal{R}(\alpha, \beta, \gamma) \cdot \mathcal{R}(0, 0, \pi) \cdot \mathcal{R}(\phi, -\theta, 0)$ , the north pole goes to  $(\theta', \phi')$ . But, we also know that we can bring the north pole to  $(\theta', \phi')$ , by the rotation  $\mathcal{R}(0, 0, \pi) \cdot \mathcal{R}(\phi', -\theta', 0)$ . Accounting for the fact that the north pole remains invariant under arbitrary rotations about the  $z$ -axis (which we take to be equal to  $\mathcal{R}(0, 0, \psi')$ ), we must have:

$$\begin{aligned} \mathcal{R}(0, 0, \pi) \cdot \mathcal{R}(\phi', -\theta', 0) \cdot \mathcal{R}(0, 0, \psi') \\ = \mathcal{R}(\alpha, \beta, \gamma) \cdot \mathcal{R}(0, 0, \pi) \cdot \mathcal{R}(\phi, -\theta, 0) \end{aligned}$$

Or, equivalently we can invert both sides to get:

$$\begin{aligned} \Leftrightarrow \mathcal{R}(-\psi', 0, 0) \cdot \mathcal{R}(0, \theta', -\phi') \cdot \mathcal{R}(-\pi, 0, 0) \\ = \mathcal{R}(0, \theta, -\phi) \cdot \mathcal{R}(-\pi, 0, 0) \cdot \mathcal{R}(-\gamma, -\beta, -\alpha) \end{aligned}$$

We have thus managed to relate the rotation  $\mathcal{R}(0, \theta, -\phi)$  to the rotation  $\mathcal{R}(0, \theta', -\phi')$ . We can use this relation to find the transformation rule for the monopole harmonics. From Eq. 4 and Eq. 5, the L.H.S. gives us:

$$\begin{aligned} D_{Q, m}^l(\mathcal{R}(-\psi', 0, 0) \cdot \mathcal{R}(0, \theta', -\phi') \cdot \mathcal{R}(-\pi, 0, 0)) \\ = \langle l, Q | e^{i\psi' J_z} \mathcal{R}(0, \theta', -\phi') e^{i\pi J_z} | l, m \rangle \\ = \sqrt{\frac{4\pi}{2l+1}} (-1)^m e^{iQ\psi'} Y_{Q, l, m}(\theta', \phi'). \end{aligned}$$

Similarly, the R.H.S. gives us (recall,  $D_{m, m'}^l(\mathcal{R}) = [D_{m', m}^l(\mathcal{R}^{-1})]^*$ ):

$$\begin{aligned} D_{Q, m}^l(\mathcal{R}(0, \theta, -\phi) \cdot \mathcal{R}(-\pi, 0, 0) \cdot \mathcal{R}(-\gamma, -\beta, -\alpha)) \\ = \sum_{m'} (-1)^{m'} D_{Q, m'}^l(\mathcal{R}(0, \theta, -\phi)) D_{m', m}^l(\mathcal{R}(-\gamma, -\beta, -\alpha)) \\ = \sqrt{\frac{4\pi}{2l+1}} \sum_{m'} (-1)^{m'} Y_{Q, l, m'}(\theta, \phi) [D_{m, m'}^l(\mathcal{R}(\alpha, \beta, \gamma))]^*. \end{aligned}$$

Therefore, we find that under a rotation  $\mathcal{R}(\alpha, \beta, \gamma)$ , which takes the point  $(\theta, \phi)$  to the point  $(\theta', \phi')$ , the

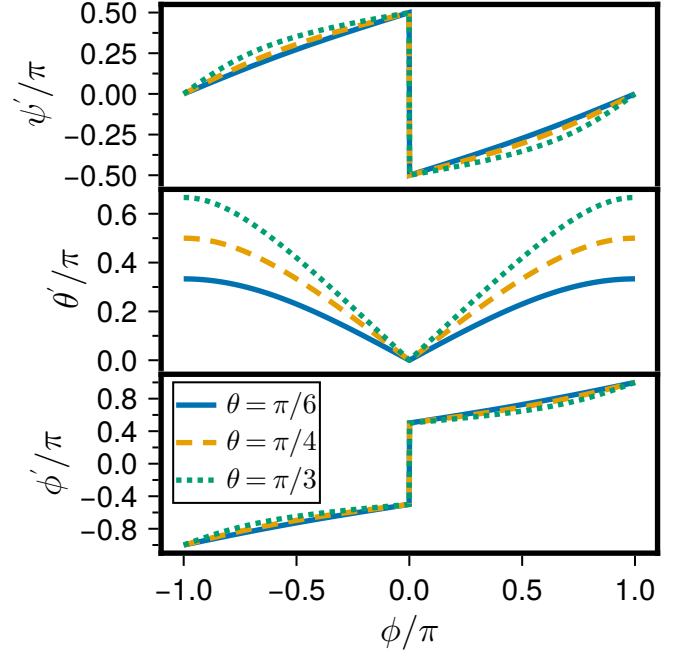


FIG. 1. In the top row, for rotations  $\mathcal{R}(\alpha = 0, \beta = -\theta, \gamma = 0)$  that take the points  $\Omega = (\theta, 0)$  to the north pole, we have plotted the angle  $\psi'$  as a function of the original azimuthal angle  $\phi$  for points initially along the  $\theta$  latitude. (The phase acquired by monopole harmonics  $Y_{Q, l, m}(\theta, \phi)$  under rotation is  $Q\psi'$ .) In the middle and bottom rows, we plot, for reference,  $\theta'$  and  $\phi'$  coordinates of these points after rotation.

monopole harmonics  $Y_{Q, l, m}(\theta, \phi)$  transform as:

$$\begin{aligned} Y_{Q, l, m}(\theta', \phi') \\ = e^{-iQ\psi'} \sum_{m'=-l}^l (-1)^{m-m'} [D_{m, m'}^l(\alpha, \beta, \gamma)]^* Y_{Q, l, m'}(\theta, \phi). \end{aligned} \quad (6)$$

We thus find that in Eq. 2, the unitary matrix  $U_{m, m'}^l$  is equal to  $(-1)^{m-m'} [D_{m, m'}^l(\alpha, \beta, \gamma)]^*$  and the phase  $\Gamma$  is equal to  $-Q\psi'$  with  $\psi'$  determined numerically from:

$$\mathcal{R}(0, 0, \psi') = \mathcal{R}(0, \theta', -\phi') \cdot \mathcal{R}(\alpha - \pi, \beta, \gamma + \pi) \cdot \mathcal{R}(\phi, -\theta, 0) \quad (7)$$

We present solutions for  $\psi'$  in Fig. 1 and Fig. 2 for some parameter choices, which demonstrate that  $\psi'$  in general depends on  $(\theta, \phi)$  and  $\mathcal{R}(\alpha, \beta, \gamma)$  in a complicated manner and is discontinuous at points which go to the poles under the rotation  $\mathcal{R}(\alpha, \beta, \gamma)$ . A priori, we expect such a discontinuity at points that go to the poles due to the presence of Dirac strings (recall that the Dirac strings are fixed to the poles of the co-ordinate system).

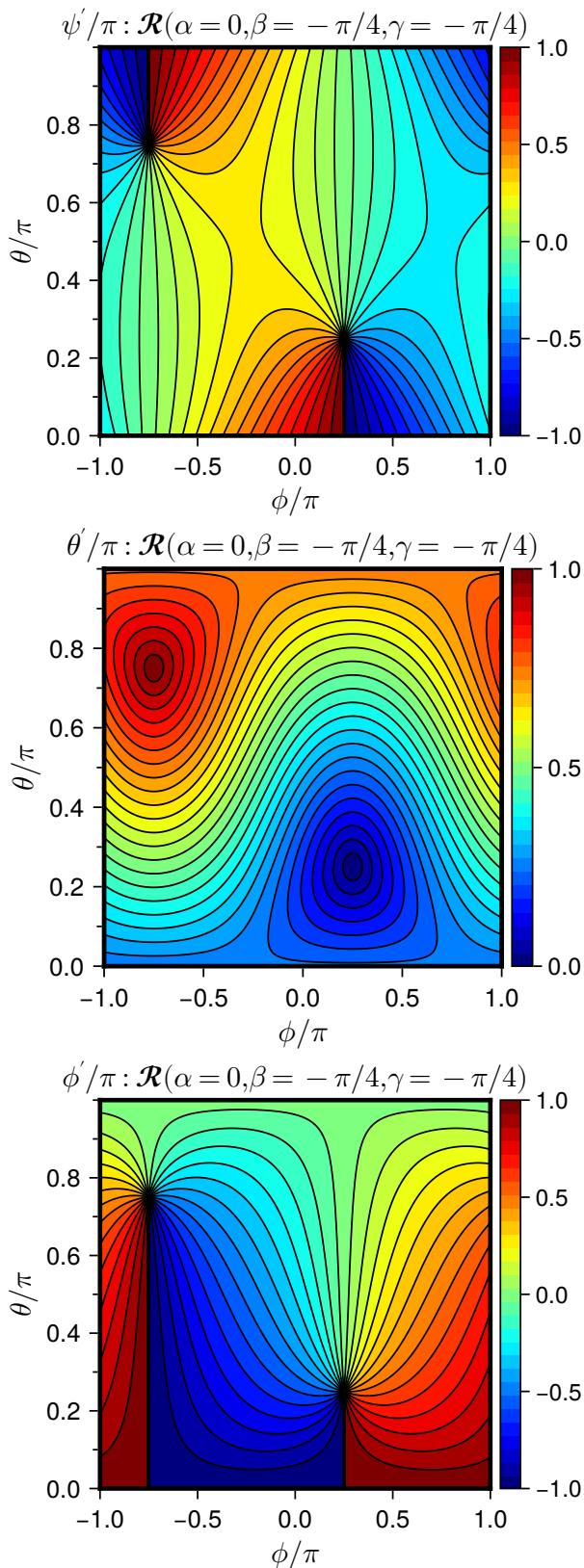


FIG. 2. For the rotation  $\mathcal{R}(\alpha=0, \beta=-\pi/4, \gamma=-\pi/4)$ , we plot  $\psi'$ ,  $\theta'$  and  $\phi'$  as a function of the initial coordinates  $(\theta, \phi)$  over the entire sphere.

## II. JAIN-KAMILLA PROJECTION IN TERMS OF UNIT QUATERNIONS

In this section, we first review the traditional formulation of the Jain-Kamilla (JK) projection method, which provides a variational ansatz for the lowest Landau level (LLL) projected composite fermion (CF) wave functions. We then derive a novel reformulation of the JK projection employing the quaternion formulation of the monopole harmonics. We discuss its practical implementation and show that the quaternion formulation dramatically increases the computational speed and accuracy of JK projected wave functions, making it possible to study Jain FQH states at fillings  $\nu = 1/3, 2/5, \dots, 20/41$  and  $\nu = 2/3, 3/5, \dots, 19/37, 20/39$ .

A crucial ingredient of the wave functions of CFs is the  $P_{\text{LLL}}$  operator in their definition (for a brief review, see Sec. III or Ref. [3]). Therefore, performing the LLL projection efficiently is vital in the numerical studies of CFs. (The unprojected wave functions have occupation of higher Landau levels but they **do** not describe the physics of Landau level mixing. Even for describing the physics of LL mixing, one begins with the LLL wave function [6, 7].) To this end, Jain and Kamilla [8] proposed an ansatz for the LLL projected CF wave functions:

$$\begin{aligned}
 & P_{\text{LLL}} \det [Y_{Q^*, l_j, m_j}(\Omega_i)] \prod_{a < b=1}^N (u_a v_b - u_b v_a)^2 \\
 & \rightarrow \det \left[ P_{\text{LLL}} Y_{Q^*, l_j, m_j}(\Omega_i) \prod_{k \neq i} (u_i v_k - u_k v_i) \right]
 \end{aligned} \tag{8}$$

In the JK projected wave functions, the problem of projecting an  $N$ -particle wave function into the LLL, which has an  $\mathcal{O}(N^N)$  complexity (recall that a Landau level has a macroscopic degeneracy), is reduced to projecting each element  $Y_{Q^*, l_j, m_j}(\Omega_i) \prod_{k \neq i} (u_i v_k - u_k v_i)$  of a Slater determinant that contains at most one particle outside the LLL, which has an overall complexity  $\mathcal{O}(N^{2-3})$ . This makes it possible to study systems with  $N$  up to a few hundred electrons, thus allowing for a quantitative understanding of the thermodynamic properties of many FQH states.

Traditionally, the LLL projection of the elements of the determinant in the JK projected wave function is carried out as follows. First note that in  $Y_{Q^*, l_j, m_j}(\Omega_i) \prod_{k \neq i} (u_i v_k - u_k v_i)$  only the state of the  $i^{\text{th}}$  electron is possibly outside the LLL. We thus need to project wave functions of the form:  $Y_{Q^*, l, m}(\Omega) \left( \sum_{m=-Q_1}^{Q_1} c_m Y_{Q_1, Q_1, m}(\Omega) \right)$  where  $c_m$  are arbitrary complex numbers and  $Q_1 = (N-1)/2$ . This can

be accomplished as follows [3]:

$$\begin{aligned} P_{\text{LLL}} Y_{Q^*,l,m}(\Omega) & \left( \sum_{m=-Q_1}^{Q_1} c_m Y_{Q_1,Q_1,m}(\Omega) \right) \\ & = \hat{Y}_{Q^*,l,m}^{Q_1}(\Omega) \left( \sum_{m=-Q_1}^{Q_1} c_m Y_{Q_1,Q_1,m}(\Omega) \right). \end{aligned} \quad (9)$$

Here,  $\hat{Y}_{Q^*,l,m}^{Q_1}(\Omega)$  is an operator *independent* of the LLL state it acts on, and can be obtained (up to a proportionality constant) by moving the  $u^*$ 's and  $v^*$ 's in each term of the polynomial expression for  $Y_{Q^*,l,m}(\Omega)$  (given in Eq. 1) to the *right* and then replacing them with  $\partial/\partial u$  and  $\partial/\partial v$  respectively. That is:

$$\begin{aligned} P_{\text{LLL}} Y_{Q^*,l,m}(\Omega_i) \prod_{k \neq i} (u_i v_k - u_k v_i) & \propto \\ \sum_s (-1)^s \binom{l-m}{s} \binom{Q^*+l}{l-m-s} u_i^{Q^*+m+s} v_i^{l-m-s} & \times \\ \left[ \left( \frac{\partial^s}{\partial u_i^s} \right) \left( \frac{\partial^{l-Q^*-s}}{\partial v_i^{l-Q^*-s}} \right) \right] \prod_{k \neq i} & (u_i v_k - u_k v_i). \end{aligned} \quad (10)$$

The mixed derivatives  $\partial_{u_i}^s \partial_{v_i}^{l-Q^*-s} \prod_{k \neq i} (u_i v_k - u_k v_i)$  in the traditional formulation are the biggest hurdle in the numerical evaluation of the JK projected wave functions. Firstly, the number of such derivatives that need to be evaluated grows quadratically with  $l_{\text{max}} - Q^*$  ( $l_{\text{max}}$  is the maximum angular momentum of an electron in  $\det Y_{Q^*,l_j,m_j}(\Omega_i)$ ) as  $(l_{\text{max}} - Q^* + 1)(l_{\text{max}} - Q^* + 2)/2$ . This makes it impractical (see Fig. 4 and Fig. 5) to study any parallel-flux attached CF states for fillings  $\nu > 8/17$  (and any reverse-flux attached CF states containing more than  $\sim 40$  particles). Secondly, even when the number of derivatives required is manageable, no numerically stable algorithm is known to compute them (see Ref. [9] for a discussion). This can be seen from Fig. 3 where we show the accuracy in the evaluation of the wave function (evaluated using the method outlined in Ref. [3]) for various values of  $n = l_{\text{max}} - Q^*$  and system sizes. We find that for  $n \geq 8$ , within the standard double-precision arithmetic, the loss in accuracy makes numerical studies infeasible. Although it is possible to get accurate wave functions using higher precision arithmetic [10] as seen in Fig. 3, it leads to a dramatic decrease in speed as seen from Fig. 6 rendering it impractical. To overcome these limitations, we now propose a new formulation based on the quaternion representation of monopole harmonics; within this formulation the computation of the CF wave functions scales linearly with  $l_{\text{max}} - Q^*$  and is numerically stable.

We begin by extending the JK projected wave functions to the space of unit quaternions, i.e., we replace  $Y_{Q^*,l,m}(\Omega_i)$  with  $\mathcal{Y}_{Q^*,l,m}(r_i)$  where  $r_i = e^{\phi_i \mathbf{k}/2} e^{\theta_i \mathbf{y}/2} e^{\psi_i \mathbf{k}/2}$  (or equivalently,  $u_i, v_i$  with the sym-

metric and anti-symmetric projections  $r_{S_i}, r_{A_i}$ ) in Eq. 10:

$$\det \left[ P_{\text{LLL}} \mathcal{Y}_{Q^*,l_j,m_j}(r_i) \prod_{k \neq i} (r_{S_i} r_{A_k} - r_{S_k} r_{A_i}) \right]. \quad (11)$$

Using  $r_i^{-1} = r_i^* S$  and  $r_i^{-1} A = -r_i A$ , we note that the symmetric and anti-symmetric projections transform under quaternion multiplication as

$$(r_i^{-1} \cdot r_j)_S = r_i^* S r_j S + r_i^* A r_j A,$$

and

$$(r_i^{-1} \cdot r_j)_A = r_i S r_j A - r_i A r_j S.$$

We can define a ‘‘quaternion displacement’’  $d(r_i, r_j) = (r_i^{-1} \cdot r_j)_A = r_i S r_j A - r_i A r_j S$ . Like the planar displacement  $z_i - z_j$  (here,  $z_i = x_i - y_i$ ) which is invariant under translations  $z_i \rightarrow z_i + z$ , the quaternion displacement  $d(r_i, r_j)$  is invariant under left quaternion multiplication i.e.  $d(r \cdot r_i, r \cdot r_j) = d(r_i, r_j) \forall r!$  We now leverage this invariance as follows:

$$\begin{aligned} \mathcal{Y}_{Q^*,l,m}(r_i) \prod_{j \neq i} d(r_i, r_j) & = \sum_{m'=-l}^l \mathcal{D}_{m,m'}^l(r) \times \\ \mathcal{Y}_{Q^*,l,m'}(r^{-1} \cdot r_i) \prod_{j \neq i} [(r^{-1} \cdot r_i)^{-1} \cdot (r^{-1} \cdot r_j)]_A. \end{aligned}$$

Given that this is true for all  $r$ , we must have:

$$\begin{aligned} P_{\text{LLL}} \mathcal{Y}_{Q^*,l,m}(r_i) \prod_{j \neq i} d(r_i, r_j) & = \sum_{m'=-l}^l \mathcal{D}_{m,m'}^l(r) \times \\ P_{\text{LLL}} \left\{ \mathcal{Y}_{Q^*,l,m'}(r^{-1} \cdot r_i) \prod_{j \neq i} [(r^{-1} \cdot r_i)^{-1} \cdot (r^{-1} \cdot r_j)]_A \right\}. \end{aligned}$$

Now, let  $R_i = r^{-1} \cdot r_i$  and  $R_{S_i}, R_{A_i}$  be the corresponding symmetric and anti-symmetric projections. It then follows that:

$$\begin{aligned} P_{\text{LLL}} \left\{ \mathcal{Y}_{Q^*,l,m'}(r^{-1} \cdot r_i) \prod_{j \neq i} [(r^{-1} \cdot r_i)^{-1} \cdot (r^{-1} \cdot r_j)]_A \right\} \\ = P_{\text{LLL}} \mathcal{Y}_{Q^*,l,m'}(R_i) \prod_{j \neq i} (R_{S_i} R_{A_j} - R_{S_j} R_{A_i}) \\ = \left( \prod_{j \neq i} R_{A_j} \right) \times \\ P_{\text{LLL}} \mathcal{Y}_{Q^*,l,m'}(R_i) \sum_{r=0}^{N-1} (-1)^r R_{S_i}^{(N-1)-r} R_{A_i}^r e_r \left( \left\{ \frac{R_{S_j}}{R_{A_j}} \right\}_{j \neq i} \right). \end{aligned}$$

Here,  $e_r(X)$  is the  $r^{\text{th}}$  elementary symmetric polynomial constructed from the elements of the set  $X$ . We now

have:

$$\begin{aligned} & P_{\text{LLL}} \mathcal{Y}_{Q^*, l, m'}(R_i) \sum_{r=0}^{N-1} (-1)^r R_{S_i}^{(N-1)-r} R_{A_i}^r e_r \left( \left\{ \frac{R_{S_j}}{R_{A_j}} \right\}_{j \neq i} \right) \\ &= \sum_{m''=-Q_1}^{Q_1} \frac{1}{\sqrt{\frac{2Q_1+1}{4\pi} \binom{2Q_1}{Q_1-m''}}} e_{Q_1-m''} \left( \left\{ \frac{R_{S_j}}{R_{A_j}} \right\}_{j \neq i} \right) \times \\ & P_{\text{LLL}} \mathcal{Y}_{Q^*, l, m'}(R_i) \mathcal{Y}_{Q_1, Q_1, m''}(R_i). \end{aligned}$$

Up until now, everything has involved rotations by an arbitrary quaternion  $r$ . Now, *and this is the key step*, we make a specific choice:  $r = r_i^{-1}$  such that  $R_i = \mathbf{1}$ . Here the monopole harmonics satisfy  $\mathcal{Y}_{Q, Q, m'}(\mathbf{1}) = \delta_{m', Q} \sqrt{(2Q+1)/(4\pi)}$ . And thus when  $R_i = \mathbf{1}$ ,  $P_{\text{LLL}} \mathcal{Y}_{Q^*, l, m'}(R_i) \mathcal{Y}_{Q_1, Q_1, m''}(R_i)$  is non-zero if and only if  $m'' + m' = Q^* + Q_1$ . This follows by noting that we can write  $\mathcal{Y}_{Q^*, l, m'}(R_i) \mathcal{Y}_{Q_1, Q_1, m''}(R_i)$  as  $\sum_L c_L \mathcal{Y}_{Q_1+Q^*, L, m'+m''}(R_i)$  [3]. Therefore, we have:

$$\begin{aligned} & P_{\text{LLL}} \mathcal{Y}_{Q^*, l, m'}(R_i) \sum_{r=0}^{N-1} (-1)^r R_{S_i}^{(N-1)-r} R_{A_i}^r e_r \left( \left\{ \frac{R_{S_j}}{R_{A_j}} \right\}_{j \neq i} \right) \\ &= \frac{1}{\sqrt{\frac{2Q_1+1}{4\pi} \binom{2Q_1}{m'-Q^*}}} e_{m'-Q^*} \left( \left\{ \frac{(r_i^{-1} \cdot r_j)_S}{(r_i^{-1} \cdot r_j)_A} \right\}_{j \neq i} \right) \times \\ & [P_{\text{LLL}} \mathcal{Y}_{Q^*, l, m'}(r) \mathcal{Y}_{Q_1, Q_1, Q^*+Q_1-m'}(r)]_{r \rightarrow \mathbf{1}}. \end{aligned}$$

Let us note that [3]

$$\begin{aligned} & P_{\text{LLL}} \mathcal{Y}_{Q^*, l, m'}(r) \mathcal{Y}_{Q_1, Q_1, Q^*+Q_1-m'}(r) \\ &= (-1)^{l+2Q_1+Q^*} \\ & \times \sqrt{\frac{(2l+1)(2Q_1+1)(2Q_1+2Q^*+1)}{4\pi}} \\ & \times \begin{pmatrix} l & Q_1 & Q_1+Q^* \\ -m' & m'-Q_1-Q^* & Q_1+Q^* \end{pmatrix} \\ & \times \begin{pmatrix} l & Q_1 & Q_1+Q^* \\ Q^* & Q_1 & -Q^*-Q_1 \end{pmatrix} \mathcal{Y}_{Q^*+Q_1, Q^*+Q_1, Q^*+Q_1}(r). \end{aligned}$$

Here, the  $2 \times 3$  matrices correspond to the  $3j$  symbols, which can be calculated conveniently via a symbolic manipulation software to obtain:

$$\begin{aligned} & \frac{(P_{\text{LLL}} \mathcal{Y}_{Q^*, l, m'}(r) \mathcal{Y}_{Q_1, Q_1, Q^*+Q_1-m'}(r))_{r \rightarrow \mathbf{1}}}{\sqrt{\frac{2Q_1+1}{4\pi} \binom{2Q_1}{m'-Q^*}}} \\ &= (-1)^{m'-Q^*} \sqrt{\frac{2l+1}{4\pi} \frac{(2Q_1+2Q^*+1)!}{(2Q_1+Q^*+l+1)!}} \\ & \times \frac{(2Q_1+Q^*-m')!}{(2Q_1+Q^*-l)!} \sqrt{\frac{(l-Q^*)! (l+m')!}{(l-m')! (l+Q^*)!}}. \end{aligned}$$

We therefore find that the elements of the Slater determinant in the JK wave function (see Eq. 10) are equal

to:

$$\begin{aligned} & \left[ P_{\text{LLL}} \mathcal{Y}_{Q^*, l, m}(r_i) \prod_{j \neq i} d(r_i, r_j) \right] / \prod_{j \neq i} d(r_i, r_j) \\ &= \sum_{m'=Q^*}^l (-1)^{m'-Q^*} N_{m', Q^*, Q_1}^l \mathcal{D}_{m, m'}^l(r_i) \tilde{e}_{m'-Q^*}(X_i) \\ & N_{m', Q^*, Q_1}^l \\ &= \left( \binom{2Q_1}{l-Q^*} \binom{l-Q^*}{m'-Q^*} / \binom{2Q_1+l+Q^*+1}{l-Q^*} \right) \\ & \times \sqrt{\binom{2l}{l+Q^*} / \binom{2l}{l+m'}} \times \sqrt{(2l+1)/(4\pi)}. \end{aligned} \tag{12}$$

Here,  $\tilde{e}_r(X_i) \equiv e_r(X_i)/\binom{N-1}{r}$  are a regularized version of the elementary symmetric polynomials  $e_{m'-Q^*}(X_i)$ .  $X_i$  is the set  $\{(r_i^{-1} \cdot r_j)_S / (r_i^{-1} \cdot r_j)_A | j \neq i, j = 1, \dots, N\}$ . Importantly, if  $l_{\text{max}}$  is the maximum angular momentum of an electron in  $\det[Y_{Q, l_j, m_j}(r_i)]$ , we need to evaluate only  $l_{\text{max}} - Q^* + 1$  elementary symmetric polynomials (for each column)! The elementary symmetric polynomials themselves can be computed very efficiently by a dynamic programming algorithm [9, 11] that leverages the following relationship:  $e_k(\{x_1, x_2, \dots, x_N\}) = e_{k-1}(\{x_2, \dots, x_N\}) + x_1 e_{k-1}(\{x_2, \dots, x_N\})$ . Given that the elements of the set  $X_i$ , for example, equal to  $\{(u_i^* u_j + v_i^* v_j) / (u_i v_j - u_j v_i) | j \neq i\}$  on the  $\psi_i = 0$  sub-space, are well-behaved (during a Monte Carlo run with the sampling distribution as the wavefunction) because of the Pauli principle, it follows that the (regularized) elementary symmetric polynomials appearing in Eq. 12 can always be safely computed within standard double-precision arithmetic. Further, from the Fourier decomposition of Wigner- $d$  matrices proposed in Ref. [12],

$$\begin{aligned} & d_{m, m'}^l(\theta) = \langle l, m | e^{-i\theta J_y} | l, m' \rangle \\ &= \langle l, m | \left( \sum_{\mu'} y | l, \mu' \rangle \langle l, \mu' | y \right) e^{-i\theta J_y} \\ & \times \left( \sum_{\mu} y | l, \mu \rangle \langle l, \mu' | y \right) | l, m' \rangle \\ &= \sum_{\mu=-l}^l e^{-i\mu\theta} \langle l, m | l, \mu \rangle_{yy} \langle l, \mu | l, m' \rangle \end{aligned}$$

where  $|l, \mu\rangle_y$  are the eigenstates of  $J_y$  (obtained through exact diagonalization of  $J_y$  in the  $J_z$  eigenstate basis), we can calculate the Wigner- $\mathcal{D}$  matrices appearing in Eq. 12 to an accuracy of  $10^{-14}$  (for  $l_{\text{max}} \leq 100$ ). The accuracy in calculating the elementary symmetric polynomials and the Wigner- $\mathcal{D}$  matrices, alongside the linear scaling in  $l_{\text{max}} - Q^*$  leads to a dramatic increase in both the speed and accuracy of the evaluation of the JK projected

wave functions as seen from Fig. 3, Fig. 4, Fig. 5 and Fig. 6. This allows us to study for the first time any Jain FQH state at filling  $\nu$  in the range  $10/21, \dots, 20/41$  or  $20/39, \dots, 6/11$ . Further, even for fillings previously accessible, our new method allows us to access much larger system sizes than before, paving the way for studying the thermodynamic behavior of observables with complicated or unknown system size dependence.

### III. MAGNETO-ROTON MODES OF JAIN FQH STATES

In this section, we briefly review the Jain  $\nu = n/(2pn + 1)$  states and their lowest energy charged and neutral excitations (the latter are also referred to as the magneto-roton modes) in the spherical geometry. To explore the possibility of a magneto-roton instability of the FQHE along the sequence  $\nu = n/(2n + 1)$  for large  $n$ , we have evaluated the excitation energies of the magneto-roton modes for fillings  $\nu = 1/3, 2/5, \dots, 10/21$  and  $\nu = 15/31$  using our new formulation. These results show no evidence of a magneto-roton instability.

Electrons constrained to move within the LLL (for filling factors  $\nu \leq 1$ ) capture  $2p$  (here,  $p \in \mathbb{Z}^+$ ) vortices to form CFs. As a result of the vortex capture, CFs experience a reduced magnetic field  $B^* = B - 2p\rho\phi_0$ . Here,  $B$  is the applied magnetic field, and  $\rho$  is the electron density. CFs experiencing the reduced field  $B^*$  inhabit Landau-like levels called  $\Lambda$  levels (ALs) that are separated by a nearly constant energy difference called the CF cyclotron energy  $\hbar\omega_c^* \propto B^*$ . When CFs fill the first  $n$  CF LLs (called  $\Lambda$  levels), corresponding to electrons at filling  $\nu = n/(2pn + 1)$ , the system becomes incompressible. (Note, that by definition the filling factor  $\nu^*$  of CFs is related to the electronic filling as  $\nu^* = \nu/(1 - 2p\nu) \Leftrightarrow \nu = \nu^*/(1 + 2p\nu^*)$ .) That is, the integer quantum Hall effect (IQHE) of CFs results in the FQHE of electrons. An incompressible state of  $N$  CFs at monopole strength  $Q^* = N/2n - n/2$  filling  $n$  ALs (i.e.  $\nu^* = n$ ) can be written as

$$\begin{aligned} & \Psi_{n/(2pn+1)}(\Omega_1, \dots, \Omega_N) \\ &= P_{\text{LLL}} \phi_n(\Omega_1, \dots, \Omega_N) \times [\phi_1(\Omega_1, \dots, \Omega_N)]^{2p} \\ & \phi_1(\Omega_1, \dots, \Omega_N) = \prod_{i < j=1}^N (u_i v_j - u_j v_i). \end{aligned} \quad (13)$$

Here,  $\Omega_i \equiv (\theta_i, \phi_i)$  is the position of the  $i^{\text{th}}$  electron on the sphere and  $u_i, v_i$  the corresponding spinor variables.  $P_{\text{LLL}}$  is the projection operator into the LLL.  $\phi_n(\Omega_1, \dots, \Omega_N)$  is a Slater determinant of  $N$  electrons filling the first  $n$  Landau levels at monopole strength  $Q^*$  and  $\phi_1^{2p}$  is the Jastrow factor which attaches  $2p$  vortices to each electron and transforms them into CFs.

The lowest energy negatively charged excitation called the quasiparticle at filling  $\nu = n/(2pn + 1)$  is obtained by adding a CF to the lowest unoccupied (i.e. the  $n^{\text{th}}$ ) AL,

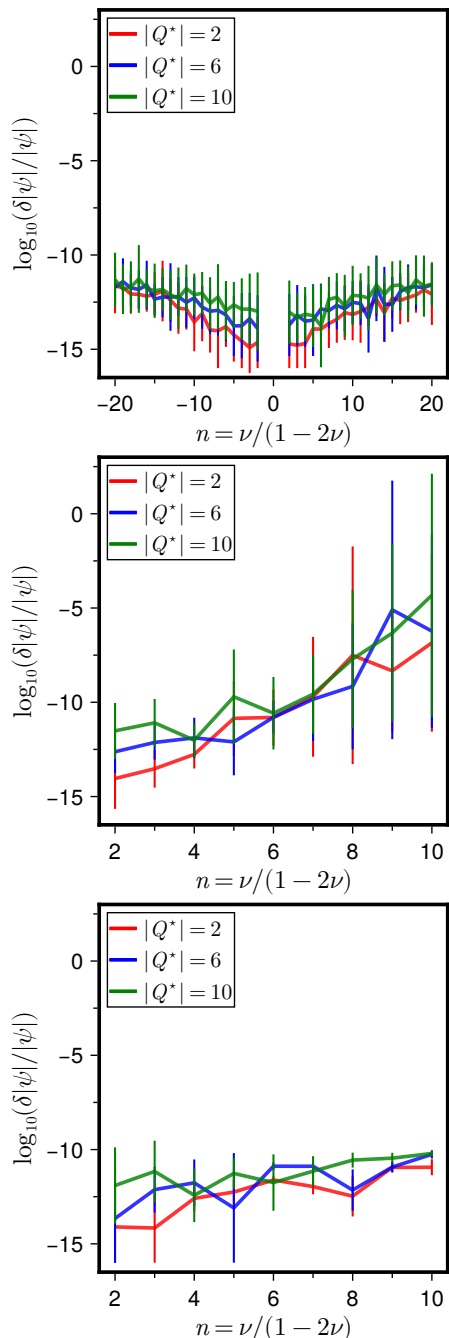


FIG. 3. The top plot shows the relative error in the (absolute value of the) Jain-Kamilla (JK) projected wave function obtained using our new formulation for the IQH states of CFs as a function of  $n$  [here we have  $n = \nu/(1 - 2\nu)$ ], and negative values of  $n$  correspond to reverse-flux attached of CFs], the number of filled  $\Lambda$  levels for three different system sizes ( $N = 2nQ^* + n^2$ ). We have calculated the “true” value of the JK projected wave function by evaluating it with higher precision arithmetic. The error bars indicate the range of the relative error over 1000 randomly generated configurations of electrons. The middle plot shows the relative error in the JK projected wave function obtained using the traditional formulation, and the bottom plot shows the same but calculated with higher precision arithmetic.

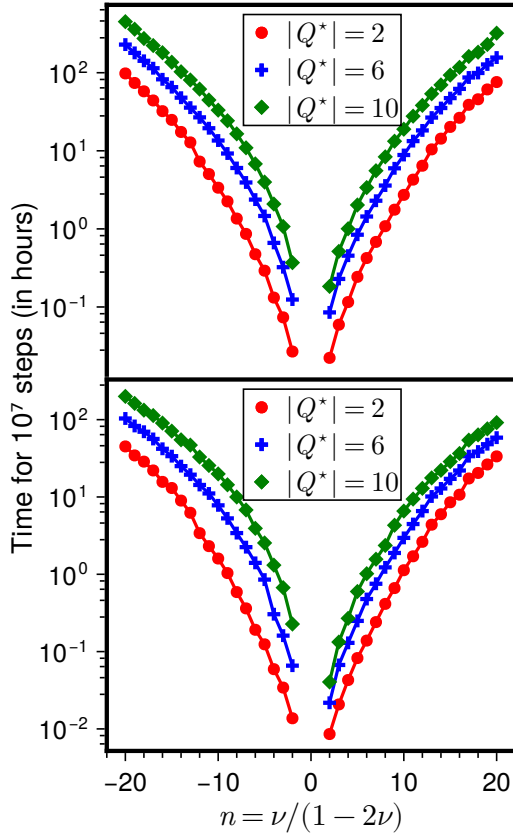


FIG. 4. In this figure, we plot the time needed to run a Monte Carlo chain of length  $10^7$  with the IQH states of CFs as the sampling wave functions as a function of  $n$ , the number of filled  $\Lambda$  levels, for three different system sizes. We generate the Monte Carlo chain according to the Metropolis-Hastings-Gibbs algorithm. The wave functions are evaluated according to our new formulation for JK projection. In the top plot, we include the time required for a “full” evaluation, which involves evaluation of the CF Slater matrix, the determinant of this matrix and its inverse. (The inverse is used in CF diagonalization [13] wherein the ratio between two JK projected wave functions is efficiently calculated using the matrix determinant lemma [14].) We show in the bottom plot the time required to evaluate only the CF Slater matrix.

and a positively charged excitation called the quasihole is obtained by removing a CF from the highest occupied (i.e. the  $(n-1)^{\text{th}}$ )  $\Lambda$ L. A state containing a CF added to the  $n^{\text{th}}$   $\Lambda$ L in the  $L_z = m$  orbital is written as

$$\begin{aligned} \Psi_{n/(2pn+1)}^{\text{qp},m}(\Omega_1, \dots, \Omega_N) \\ = P_{\text{LLL}} \phi_n^{\text{qp},m}(\Omega_1, \dots, \Omega_N) \times [\phi_1(\Omega_1, \dots, \Omega_N)]^{2p}. \end{aligned} \quad (14)$$

Here,  $Q^* = (N-1)/2n - n/2$  and  $\phi_n^{\text{qp},m}$  is a Slater determinant of  $N$  electrons filling the first  $n$  Landau levels at monopole strength  $Q^*$  and the  $L_z = m$  orbital in the  $n^{\text{th}}$  Landau level. Similarly, a state with a CF removed

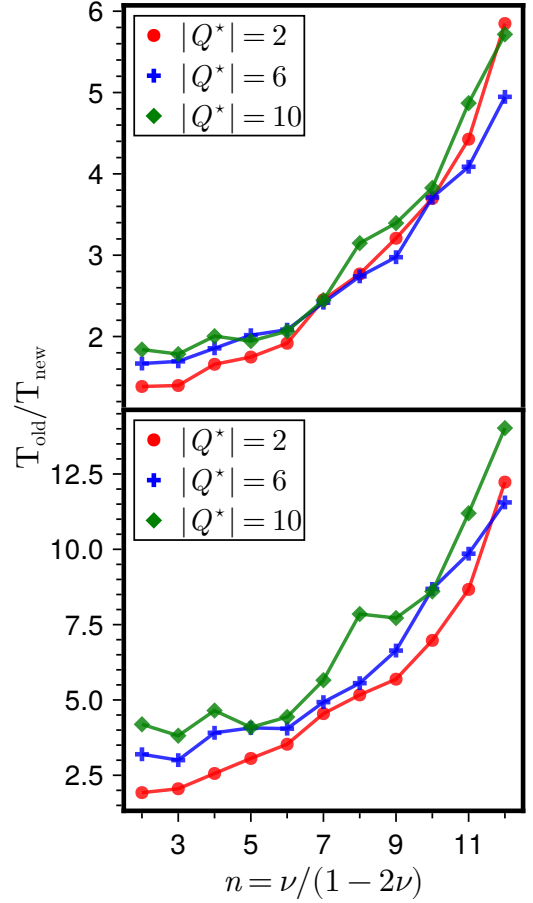


FIG. 5. In this figure, we plot the ratio of the time to run a Monte Carlo chain with the IQH states of CFs as the sampling wave functions as a function of  $n$ , the number of filled  $\Lambda$  levels (for three different system sizes) between the traditional and our new approach to JK projection. In this case, we evaluate both wave functions in the standard double precision arithmetic. The top plot, shows the ratio between times for a full evaluation and the bottom plot shows the ratio for evaluation of only the CF Slater matrix.

from the  $(n-1)^{\text{th}}$   $\Lambda$ L in the  $L_z = m$  orbital is written as

$$\begin{aligned} \Psi_{n/(2pn+1)}^{\text{qh},m}(\Omega_1, \dots, \Omega_N) \\ = P_{\text{LLL}} \phi_n^{\text{qh},m}(\Omega_1, \dots, \Omega_N) \times [\phi_1(\Omega_1, \dots, \Omega_N)]^{2p}. \end{aligned} \quad (15)$$

Here,  $Q^* = (N+1)/2n - n/2$  and  $\phi_n^{\text{qh},m}$  is a Slater determinant of  $N$  electrons filling the first  $n$  Landau levels at monopole strength  $Q^*$  except for the  $L_z = m$  orbital in the  $(n-1)^{\text{th}}$  Landau level. A CF exciton state containing a CF quasihole in the  $(n-1)^{\text{th}}$   $\Lambda$ L in the  $L_z = m$  orbital and a CF quasiparticle in  $n^{\text{th}}$   $\Lambda$ L in the  $L_z = m'$  orbital is written as

$$\begin{aligned} \Psi_{n/(2pn+1)}^{\text{ex},m,m'}(\Omega_1, \dots, \Omega_N) \\ = P_{\text{LLL}} \phi_n^{\text{ex},m,m'}(\Omega_1, \dots, \Omega_N) \times [\phi_1(\Omega_1, \dots, \Omega_N)]^{2p}. \end{aligned} \quad (16)$$

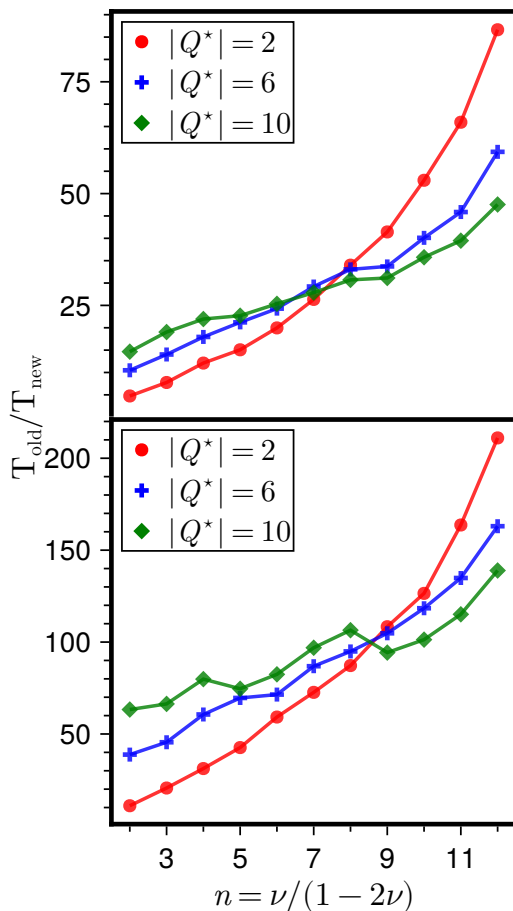


FIG. 6. In this figure, we plot the ratio of the time to run a Monte Carlo chain with the IQH states of CFs as the sampling wave functions as a function of  $n$ , the number of filled  $\Lambda$  levels between the traditional and our new approach to JK projection. In this case, we evaluate the wave function in the traditional formulation with higher precision arithmetic. The top plot, shows the ratio between times for a full evaluation and the bottom plot shows the ratio for evaluation of only the CF Slater matrix.

Here,  $\phi_n^{\text{ex},m,m'}$  is a Slater determinant containing  $N$  electrons at monopole strength  $Q^*$  filling the first  $n$  Landau levels and the  $L_z = m'$  orbital in the  $(n+1)^{\text{th}}$   $\Lambda\text{L}$ , with an electron missing from the  $L_z = m$  orbital in the  $(n-1)^{\text{th}}$   $\Lambda\text{L}$ .

The lowest energy neutral excitations i.e. the magneto-roton modes are the angular momentum eigenstates constructed from the (lowest energy) CF exciton states as:

$$\begin{aligned} & \Psi_{n/(2pn+1)}^{\text{ex},L,m}(\Omega_1, \Omega_2, \dots, \Omega_N) \\ &= \text{P}_{\text{LLL}} \left( \sum_{m_1=-l_{\text{qh}}}^{m=l_{\text{qh}}} \langle L, m | l_{\text{qh}}, -m_1; l_{\text{qp}}, m_1 + m \rangle \right. \\ & \quad \left. \times \phi_n^{\text{ex},m_1+m,-m_1}(\Omega_1, \dots, \Omega_N) [\phi_1(\Omega_1, \dots, \Omega_N)]^{2p} \right). \end{aligned} \quad (17)$$

Here,  $L$  (related to the planar momentum  $k$  as  $k = L/\sqrt{Q}$ ) is the angular momentum of the magneto-roton,  $m$  is its azimuthal quantum number.  $l_{\text{qh}} = Q^* + n - 1$  and  $l_{\text{qp}} = Q^* + n$  are the angular momentum of the CF QH and QP respectively.  $\langle L, 0 | l_{\text{qh}}, -m; l_{\text{qp}}, m \rangle$  are the Clebsch-Gordon coefficients.

If the CFs were completely non-interacting, the magneto-roton mode would be dispersionless with an excitation energy equal to  $\hbar\omega_c^*$  (the kinetic energy of CFs) relative to the CF integer quantum Hall (IQH) state (see Eq. 13). However, in reality, the CFs do experience a residual interaction [15], which results in a dispersion of the magneto-roton mode. Along the sequence  $\nu = n/(2n+1)$ , as the effective magnetic field felt by CFs decreases (recall  $Q^* \approx Q/(2n+1)$ ), the excitation energy of the magneto-roton mode also decreases. This raises an important question: Could the residual interaction between CFs drive a magneto-roton instability (i.e., result in a magneto-roton with negative excitation energy) for sufficiently large  $n$ ? An explicit calculation of the magneto-roton dispersion is necessary to answer this, as such an outcome cannot be ruled out a priori.

For the interaction  $\hat{V}_I = \sum_{i<j=1}^N V_I(|r_i - r_j|)$  with  $V_I = 1/|r_i - r_j|$ , we calculate the energy (recall that after LLL projection the kinetic energy of the electrons is necessarily quenched) of a wave function  $\Psi$  (either equal to  $\Psi_{n/(2n+1)}$  or  $\Psi_{n/(2n+1)}^{\text{ex},L,0}$ ) as  $\sum \left[ |\Psi/\Psi_{n/(2n+1)}|^2 \hat{V}_I \right] / \sum \left[ |\Psi/\Psi_{n/(2n+1)}|^2 \right]$ . Here,  $\sum$  is a sum over electronic configurations generated by sampling with respect to  $|\Psi_{n/(2n+1)}|^2$  according to the Metropolis-Hastings-Gibbs algorithm following our new method for JK projection. We generate  $\approx 1.5 \times 10^7$  samples across 100 Monte Carlo chains to calculate the excitation energy  $\Delta E$  (i.e. the energy wrt to  $\Psi_{n/(2n+1)}$ ) of magneto-roton modes in Fig. 7 and estimate the error using the Jackknife resampling technique [16]. To eliminate some of the system-size dependence in our results, we account for the density correction [17] i.e. place the electrons on a sphere of radius  $\sqrt{N/(2\nu)}\ell$  in the calculation of  $\Delta E$ .

As can be seen from Fig. 7, the magneto-roton dispersions at Jain fillings  $\nu = n/(2n+1)$  reveal that as we move from  $\nu = 1/3$  to  $\nu = 1/2$ , there is a competition between the minima at  $k\ell \rightarrow 0$  and  $k\ell \rightarrow 2$  towards gap closing. For  $\nu \leq 7/15$ , the lowest energy excitation occurs at the minimum at  $k\ell \sim 2$ , but for  $\nu \geq 8/17$ , the lowest energy excitation occurs at  $k\ell \sim 0$ . Importantly, we find no evidence of magneto-roton instability for all the systems we have studied.

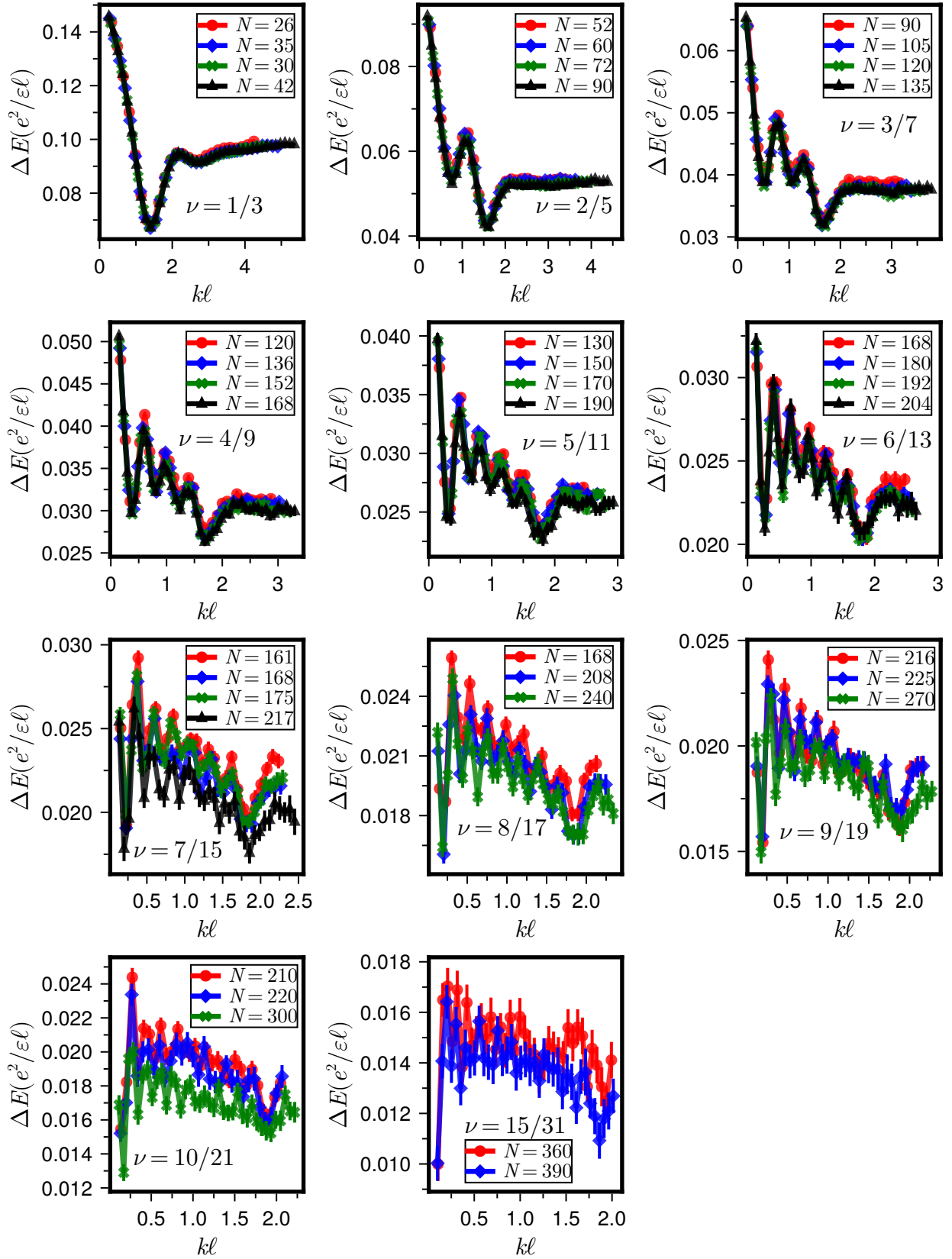


FIG. 7. This figure shows the excitation energy  $\Delta E$  of the magneto-roton modes at  $\nu = 1/3, 2/5, \dots, 10/21$  and  $\nu = 15/31$  as a function of their momentum  $k\ell$  for systems with  $N$  electrons. Vertical bars indicate Monte Carlo uncertainty.

- 
- [1] Tai Tsun Wu and Chen Ning Yang. Dirac monopole without strings: Monopole harmonics. *Nuclear Physics B*, 107(3):365–380, May 1976. ISSN 0550-3213. doi: 10.1016/0550-3213(76)90143-7. URL [http://dx.doi.org/10.1016/0550-3213\(76\)90143-7](http://dx.doi.org/10.1016/0550-3213(76)90143-7).
- [2] Tai Tsun Wu and Chen Ning Yang. Some properties of monopole harmonics. *Physical Review D*, 16(4):1018–1021, August 1977. ISSN 0556-2821. doi: 10.1103/physrevd.16.1018. URL <http://dx.doi.org/10.1103/PhysRevD.16.1018>.
- [3] J. K. Jain. *Composite Fermions*. Cambridge University Press, New York, US, 2007.
- [4] Eugen Wigner. *Gruppentheorie und ihre Anwendung auf die Quantenmechanik der Atomspektren*. Vieweg+Teubner Verlag, 1931. ISBN 9783663025559. doi:10.1007/978-3-663-02555-9. URL <http://dx.doi.org/10.1007/978-3-663-02555-9>.
- [5] J. J. Sakurai and Jim Napolitano. *Modern Quantum Mechanics*. Cambridge University Press, September 2020. ISBN 9781108473224. doi:10.1017/9781108587280. URL <http://dx.doi.org/10.1017/9781108587280>.
- [6] Yuhe Zhang, A. Wójs, and J. K. Jain. Landau-level mixing and particle-hole symmetry breaking for spin transitions in the fractional quantum hall effect. *Physical Review Letters*, 117(11), September 2016. ISSN 1079-7114. doi:10.1103/physrevlett.117.116803. URL <http://dx.doi.org/10.1103/PhysRevLett.117.116803>.
- [7] Jianyun Zhao, Yuhe Zhang, and J. K. Jain. Crystallization in the fractional quantum hall regime induced by landau-level mixing. *Physical Review Letters*, 121(11), September 2018. ISSN 1079-7114. doi: 10.1103/physrevlett.121.116802. URL <http://dx.doi.org/10.1103/PhysRevLett.121.116802>.
- [8] J. K. Jain and R. K. Kamilla. Composite fermions in the Hilbert space of the lowest electronic Landau level. *Int. J. Mod. Phys. B*, 11(22):2621–2660, 1997. doi: 10.1142/S0217979297001301.
- [9] Simon C. Davenport and Steven H. Simon. Spinful composite fermions in a negative effective field. *Phys. Rev. B*, 85:245303, Jun 2012. doi:10.1103/PhysRevB.85.245303. URL <http://link.aps.org/doi/10.1103/PhysRevB.85.245303>.
- [10] DoubleFloats.jl: math with more good bits. URL <https://github.com/JuliaMath/DoubleFloats.jl>.
- [11] Ian Grant Macdonald. *Symmetric Functions and Hall Polynomials*. Oxford: Clarendon Press, 1979.
- [12] X. M. Feng, P. Wang, W. Yang, and G. R. Jin. High-precision evaluation of wigner’s  $d$  matrix by exact diagonalization. *Phys. Rev. E*, 92:043307, Oct 2015. doi: 10.1103/PhysRevE.92.043307. URL <https://link.aps.org/doi/10.1103/PhysRevE.92.043307>.
- [13] Sudhansu S. Mandal and Jainendra K. Jain. Theoretical search for the nested quantum Hall effect of composite fermions. *Phys. Rev. B*, 66:155302, Oct 2002. doi: 10.1103/PhysRevB.66.155302. URL <http://link.aps.org/doi/10.1103/PhysRevB.66.155302>.
- [14] David A. Harville. *Matrix Algebra From a Statistician’s Perspective*. Springer New York, 1997. ISBN 9780387226774. doi:10.1007/b98818. URL <http://dx.doi.org/10.1007/b98818>.
- [15] Ajit C. Balram, Arkadiusz Wójs, and Jainendra K. Jain. State counting for excited bands of the fractional quantum Hall effect: Exclusion rules for bound excitons. *Phys. Rev. B*, 88:205312, Nov 2013. doi: 10.1103/PhysRevB.88.205312. URL <http://link.aps.org/doi/10.1103/PhysRevB.88.205312>.
- [16] Kandethody M. Ramachandran and Chris P. Tsokos. *Bayesian estimation and inference*, page 415–459. Elsevier, 2021. ISBN 9780128178157. doi:10.1016/b978-0-12-817815-7.00010-5. URL <http://dx.doi.org/10.1016/B978-0-12-817815-7.00010-5>.
- [17] R. Morf, N. d’Ambrumenil, and B. I. Halperin. Microscopic wave functions for the fractional quantized Hall states at  $\nu = \frac{2}{5}$  and  $\frac{2}{7}$ . *Phys. Rev. B*, 34:3037–3040, Aug 1986. doi:10.1103/PhysRevB.34.3037. URL <http://link.aps.org/doi/10.1103/PhysRevB.34.3037>.